NeuroImage: Clinical 28 (2020) 102374

Contents lists available at ScienceDirect

NeuroImage: Clinical

journal homepage: www.elsevier.com/locate/ynicl

Progressive brain atrophy and clinical evolution in Parkinson's disease

Massimo Filippi[a,b,c,*], Elisabetta Sarasso[a,c], Noemi Piramide[a,c], Tanja Stojkovic[d], Iva Stankovic[d], Silvia Basaia[a], Andrea Fontana[e], Aleksandra Tomic[d], Vladana Markovic[d], Elka Stefanova[d], Vladimir S. Kostic[d], Federica Agosta[a,c]

[a] Neuroimaging Research Unit, Institute of Experimental Neurology, Division of Neuroscience, IRCCS San Raffaele Scientific Institute, Milan, Italy
[b] Neurology and Neurophysiology Units, IRCCS San Raffaele Scientific Institute, Milan, Italy
[c] Vita-Salute San Raffaele University, Milan, Italy
[d] Clinic of Neurology, School of Medicine, University of Belgrade, Belgrade, Serbia
[e] Unit of Biostatistics, Fondazione IRCCS Casa Sollievo della Sofferenza, San Giovanni Rotondo, Foggia, Italy

ARTICLE INFO

Keywords:
Parkinson's disease
Atrophy
Clinical progression
Clinical clusters

ABSTRACT

Clinical manifestations and evolution are very heterogeneous among individuals with Parkinson's disease (PD). The aims of this study were to investigate the pattern of progressive brain atrophy in PD according to disease stage and to elucidate to what extent cortical thinning and subcortical atrophy are related to clinical motor and non-motor evolution. 154 patients at different PD stages were assessed over time using motor, non-motor and structural MRI evaluations for a maximum of 4 years. Cluster analysis defined clinical subtypes. Cortical thinning and subcortical atrophy were assessed at baseline in patients relative to 60 healthy controls. Longitudinal trends of brain atrophy progression were compared between PD clusters. The contribution of brain atrophy in predicting motor, non-motor, cognitive and mood deterioration was explored. Two main PD clusters were defined: mild (N = 87) and moderate-to-severe (N = 67). Two mild subtypes were further identified: mild motor-predominant (N = 43) and mild-diffuse (N = 44), with the latter group being older and having more severe non-motor and cognitive symptoms. The initial pattern of brain atrophy was more severe in patients with moderate-to-severe PD. Over time, mild-diffuse PD patients had the greatest brain atrophy accumulation in the cortex and the left hippocampus, while less distributed atrophy progression was observed in moderate-to-severe and mild motor-predominant patients. Baseline and 1-year cortical thinning was associated with long-term progression of motor, cognitive, non-motor and mood symptoms. Cortical and subcortical atrophy is accelerated early after the onset of PD and becomes prominent in later stages of disease according to the development of cognitive, non-motor and mood dysfunctions. Structural MRI may be useful for monitoring and predicting disease progression in PD.

1. Introduction

Clinical manifestations are very heterogeneous among individuals with Parkinson's disease (PD) (Greenland et al., 2019). Clinical subtypes have been identified according to the presence of different motor signs and symptoms, cognitive decline, non-motor symptoms and behavioural disturbances (Greenland et al., 2019). Rate of disease progression is also variable: although 50% have reached key milestones of either postural instability or dementia within 4 years from diagnosis, almost a quarter have a good prognosis at 10 years (Greenland et al., 2019). The link between protein accumulation in the brain, the consequent brain damage and the variable clinical disease progression is currently under investigation in order to identify biomarkers (Filippi et al., 2020, 2018).

MRI can accurately measure changes in cerebral structures providing biomarkers for monitoring PD progression. Over the years, numerous cross-sectional MRI studies demonstrated more profound grey matter (GM) damage in fronto-temporal, parietal, occipital and limbic areas and in basal ganglia in patients with moderate to severe PD (Agosta et al., 2013a; Lewis et al., 2016; Melzer et al., 2012; Sterling et al., 2016), although some degree of structural GM alterations has been observed also in the early phase of the disease (Agosta et al., 2013b; Fereshtehnejad et al., 2017; Lewis et al., 2016; Pereira et al., 2014). A recent review analyzed and resumed longitudinal structural

* Corresponding author at: Neuroimaging Research Unit, Institute of Experimental Neurology, Division of Neuroscience, IRCCS San Raffaele Scientific Institute and Vita-Salute San Raffaele University, Via Olgettina, 60, 20132 Milan, Italy.
E-mail address: filippi.massimo@hsr.it (M. Filippi).

https://doi.org/10.1016/j.nicl.2020.102374
Received 8 June 2020; Received in revised form 8 July 2020; Accepted 4 August 2020
Available online 07 August 2020

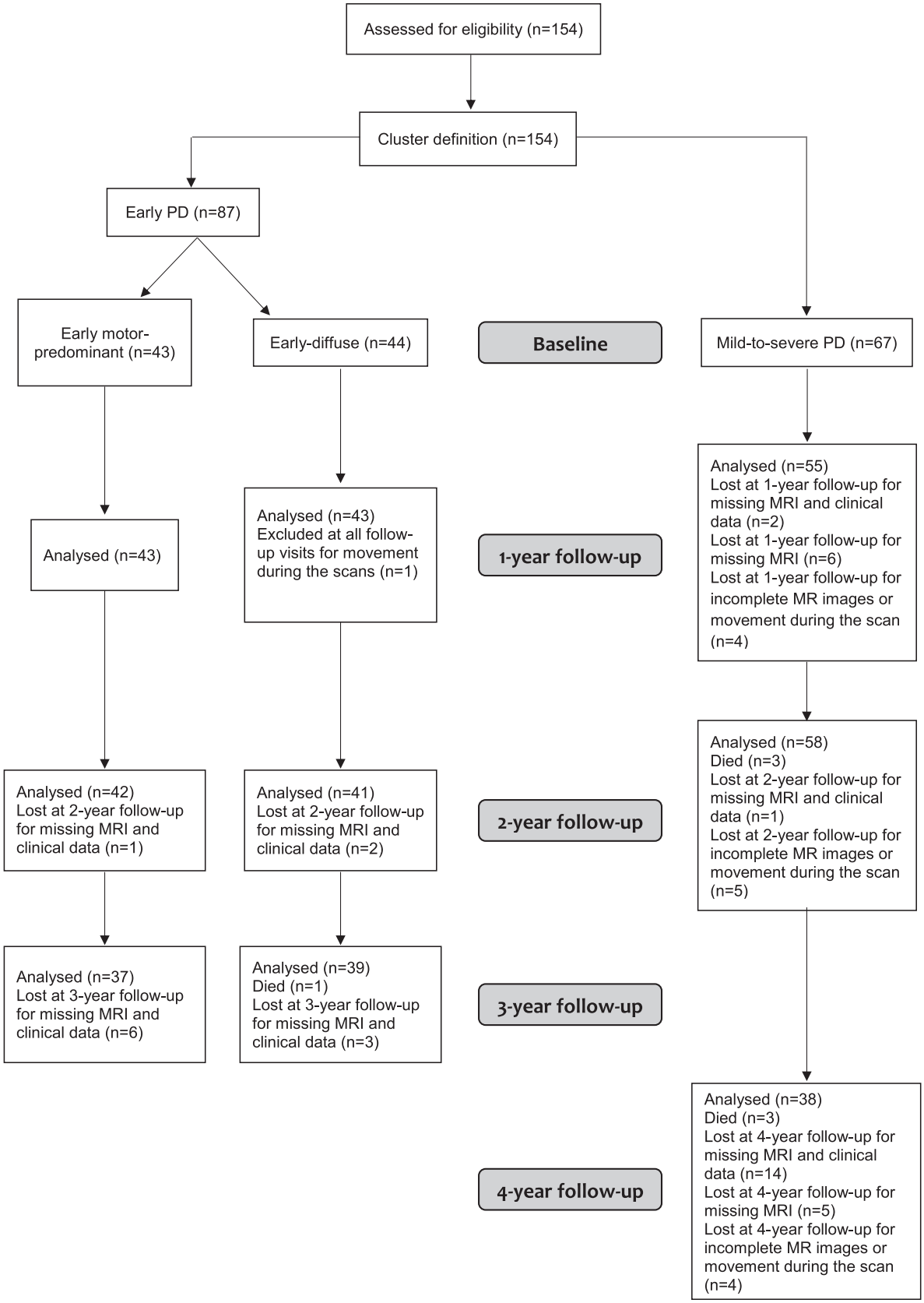

Fig. 1. Flowchart illustrating the inclusion/exclusion of Parkinson's disease (PD) subjects in the study and numbers of cases at each follow-up visit.

MRI findings in PD patients (Sarasso et al., 2020). Most consistent findings showed progressive cortical atrophy accumulation in basal ganglia, temporal/hippocampal, frontal and parietal areas in *de novo* PD cases and patients in the early/middle phase of the disease, with the achievement of a plateau in the later stage of the disease (Lewis et al., 2016; Melzer et al., 2015; Mollenhauer et al., 2016; Sampedro et al., 2019; Sarasso et al., 2020; Sterling et al., 2016; Tessa et al., 2014). Stratifying patients according to disease severity, findings are more controversial, although showing a progressive atrophy of basal ganglia over 1 year of follow-up and a widespread cortical thinning over 3–6 years in mild to moderate PD patients (Campabadal et al., 2017; Ibarretxe-Bilbao et al., 2012; Nürnberger et al., 2017; Sarasso et al., 2020). Different studies stratified patients according to cognitive impairment (Camicioli et al., 2011; Caspell-Garcia et al., 2017; Compta et al., 2013; Foo et al., 2017; Garcia-Diaz et al., 2018; Gee et al., 2017; Hanganu et al., 2014; Mak et al., 2017, 2015; Ramírez–Ruiz et al., 2005) but only few studies used prediction models showing that atrophy of the hippocampus, fronto-temporal areas, caudate, thalamus and accumbens might foresee mild cognitive impairment or dementia conversion in PD patients (Foo et al., 2017; Sarasso et al., 2020; Zhou et al., 2020). The association between brain structural changes and the evolution of other non-motor manifestations has been less explored (Baba et al., 2012; Hanganu et al., 2014; Ibarretxe-Bilbao et al., 2010; Wee et al., 2016). The main weaknesses of the majority of previous studies are the small samples, the short observation periods, the inclusion of only two timepoints, and the classification of patients that was performed according to a single variable. Such stratifying methods might not be appropriate considering the complexity of the disease. For instance, patients with more aggressive symptoms can have short disease duration and patients with long disease duration can present milder form of PD; patients with heterogeneous motor, non-motor and cognitive characteristics can present the same Hoehn and Yahr (HY) scoring; and the label “cognitive impairment” often covers a wide spectrum of cognitive features. An updated view upon the current knowledge suggests the necessity to stratify PD patients according to a combination of variables meaningful of patients’ characteristics and not according to one single feature or gross evaluation scale (Sarasso et al., 2020). To the best of our knowledge, only one longitudinal clinical study by Fereshtehnejad and colleagues used a composite model that merged numerous clinical variables including motor and non-motor domains (Fereshtehnejad et al., 2017). However, despite many attempts, there is no consensus about the best clustering model for PD patients (Mestre et al., 2018; Qian and Huang, 2019).

The present study reports a longitudinal observation of patients with PD at different disease stages assessed by comprehensive motor and non-motor serial evaluations and annual structural MRI scans over 4 years. Contrary to the majority of previous studies, our large PD cohort was followed-up by serial visits for a relatively long time period. A new cluster analysis was employed to define disease subgroups at the study entry based on demographic characteristics, disease duration, motor severity, pharmacological treatment, cognitive and non-motor features, in order to group patients with the most similar characteristics. This method was already adopted in our previous functional MRI study on the same sample (Filippi et al., 2020). Moreover, composite outcomes were used for each specific domain (motor, non-motor and cognitive). The aims of our study were to investigate the pattern of progressive brain atrophy in PD according to disease stage and subtype and to elucidate to what extent cortical thinning and subcortical atrophy are related to and can predict clinical motor and non-motor evolution.

2. Methods

2.1. Participants

Approval was received from the local ethical standards committees on human experimentation and written informed consent was obtained from all subjects prior to study participation.

154 PD patients were prospectively recruited at the Clinic of Neurology, School of Medicine, University of Belgrade, Belgrade, Serbia within the framework of an ongoing longitudinal project. Patients received a comprehensive evaluation in ON medication state including clinical, cognitive and MRI assessments at study entry and every year for a maximum of 4 years (Fig. 1). All PD patients were assessed at study entry, 1-year and 2-year follow-ups. Patients with Hoehn and Yahr (HY) < 2 were evaluated also after 3 years. After the two first follow-up visits, patients with HY ≥ 2 performed a 4-year visit as they were not able to be regularly (each year) scanned with MRI due to the severity of the symptoms or to logistic issues to move to the clinic. Patients were excluded if they had: HY > 4 and dementia (Emre et al., 2007) because they are usually less cooperative and may have some difficulties to stay still into the MRI scanner and to participate to all the study visits; moderate/severe head tremor at rest; cerebrovascular disorders (including vascular parkinsonism) or intracranial masses on routine MRI; history of traumatic brain injury; any other major neurological and medical condition; and incomplete MRI or images with artefacts. Our sample included ten patients with Glucocerebrosidase (GBA) mutation that were equally distributed among PD subgroups. Sixty age- and sex-matched healthy controls, without any neurological, psychiatric, or other disorders, were also recruited among friends and relatives of patients and by word of mouth for baseline comparison with PD patients. Healthy controls performed clinical, cognitive and MRI assessments only at baseline.

2.2. Clinical evaluation

At study entry and each follow-up visit, an experienced neurologist blinded to MRI results performed clinical assessments. Patients were examined in ON state (i.e., period when the dopaminergic medication is working and symptoms are well controlled). Demographic, general clinical and family data (sex, education, age, handedness, age at onset, side of onset, PD duration, and family history) were obtained using a semi-structured interview. Levodopa equivalent daily dose (LEDD) (Tomlinson et al., 2010) was calculated. Disease severity was defined using the HY stage score (Hoehn and Yahr, 1967) and the Unified Parkinson’s Disease Rating Scale (UPDRS) (Movement Disorder Society Task Force on Rating Scales for Parkinson's, 2003). UPDRS was used to evaluate non-motor symptoms (UPDRS I), motor symptoms (UPDRS II), motor signs (UPDRS III) and motor complications (UPDRS IV). UPDRS III rigidity, axial and bradykinesia subscores were also calculated. The severity of Freezing of Gait (FoG) was assessed using the FoG questionnaire (FoG-Q) (Giladi et al., 2000). The presence of hallucinations was reported according to the UPDRS I subscore, and of dyskinesia and fluctuations according to the UPDRS IV subscores. The presence of other non-motor symptoms (i.e., gastrointestinal, urinary, olfactory, orthostatic and sexual dysfunctions) was assessed according to the Non-Motor Symptoms questionnaire (NMS-Q) (Chaudhuri et al., 2006). Sleep disorders were investigated using the REM Sleep Behaviour Disorder Screening Questionnaire (RBDSQ) (Stiasny-Kolster et al., 2007). All these variables were obtained at each time point except for NMS-Q and RBDSQ scores, which were acquired at study entry and the last visit.

2.3. Neuropsychological and behavioural evaluations

At study entry and each follow-up visit, patients performed neuropsychological and behavioural evaluations within 48 h from MRI. The same test battery was applied in healthy controls at study entry. Evaluations were performed by expert neuropsychologists, blinded to the clinical data and MRI results as previously described (Stojkovic et al., 2018). The assessment evaluated global cognition with the Addenbrooke’s Cognitive Examination-revised (ACE-R); memory with the

Rey Auditory Verbal Learning Test (RAVLT), and the pattern (PRM) and spatial (SRM) recognition memory tests from the Cambridge Neuropsychological Test Automated Battery (CANTAB); executive functions with the digit span backward, Intra/Extra Dimensional Set Shift test (IED) from the CANTAB, and the Stroop color-word test; attention and working memory with the digit ordering test and the letter cancellation test; language with the Boston Naming Test (BNT) and the language subtest of ACE-R; fluency with semantic and phonemic fluencies; visuospatial abilities with the Hooper Visual Organization test and the visuospatial subtest of ACE-R. Mood was evaluated with the Hamilton Depression Rating Scale score (HDRS), Hamilton Anxiety Rating scale score (HAMA) and Apathy Evaluation Scale. The presence of impulsive-compulsive behaviour (ICB) was reported according to Questionnaire for Impulsive–Compulsive Disorders in Parkinson's Disease (QUIP) (Weintraub et al., 2009).

All the neuropsychological and behavioural variables were acquired at each time point except for the QUIP score, which was obtained at study entry and the last visit.

2.4. Cluster/subtype definition

Cluster analysis based on k-medoids method for data partitioning was applied on patients using the Gower distance calculated for baseline data on demographic/general clinical information (age, sex, education, age at onset, disease duration, family history), motor symptoms and signs (HY, UPDRS II-III total, UPDRS III axial and bradykinesia, presence of dyskinesia and fluctuations, FoG- Questionnaire), LEDD (Tomlinson et al., 2010), cognitive and mood data (ACE-revised, HDRS, HAMA, Apathy Evaluation Scale), and the presence of other non-motor manifestations (hallucinations, RBD, orthostatic hypotension, olfactory, gastrointestinal, urinary, sexual dysfunctions). Missing data were imputed using the Random Forest algorithm. They were very few, ranging from 0 to 1.3% for all the 29 variables.

2.5. Global composite outcomes

For analysis of clinical progression, we created four global composite outcomes (GCOs) as numeric indicators of prognosis (Fereshtehnejad et al., 2017), accounting for the most important clinical domains: motor signs/symptoms, non-motor symptoms, cognitive deficits, and mood. The four clinical domains included the following scores: 1) UPDRS-II and UPDRS-III (motor domain); 2) UPDRS I and the presence of non-motor symptoms based on the NMS-Q (non-motor domain); 3) a single test for each cognitive function according to the greatest mean rate of change for cognition – the selected cognitive tests were ACE-total (global cognition), semantic fluency (language), Intra/Extra Dimensional Set Shift (executive functions), letter cancellation test (attention) and Hooper (visuospatial function); and 4) HAMA, HDRS and Apathy Evaluation Scale (mood). For each GCO, the z-scores of each component were averaged. For calculating change (follow-up–baseline), we used the mean/standard deviation from baseline as reference (Fereshtehnejad et al., 2017). Assuming that k components (i.e. z_1, z_2, z_3, …, z_k) are needed to calculate any of the GCOs, the following formula was used:

$$\mathrm{GCO} = \mathrm{Mean}\left[\left(\frac{z_{1,FU} - z_{1,Bas}}{\mathrm{SD}(z_{1,Bas})}\right), \left(\frac{z_{2,FU} - z_{2,Bas}}{\mathrm{SD}(z_{2,Bas})}\right), \cdots, \left(\frac{z_{k,FU} - z_{k,Bas}}{\mathrm{SD}(z_{k,Bas})}\right)\right]$$

Higher GCO scores indicate worse function for motor, non-motor and mood domains, while lower GCO indicates worse cognitive performance.

2.6. MRI acquisition

Baseline and follow-up brain MRI scans were acquired on the same 1.5 Tesla Philips Medical System Achieva machine. The following MR sequences were obtained: dual-echo (DE) turbo spin-echo (repetition time [TR] = 3125 ms, echo time [TEs] = 20/100 ms, echo train length = 6, 44 axial slices, thickness = 3.0 mm, matrix size = 256 × 247, field of view [FOV] = 240 × 232 mm^2; voxel size, 0.94 × 0.94 × 3 mm^3, in-plane sensitivity encoding [SENSE] parallel reduction factor, 1.5); and high resolution 3D sagittal T1-weighted Turbo Field Echo (TFE) (frequency direction = anterior-posterior, TR = 7.1 ms, TE = 3.3 ms, inversion time = 1000 ms, flip angle = 8°, matrix size = 256 × 256 × 180 [inferior-superior, anterior-posterior], FOV = 256 × 256 mm^2, section thickness = 1 mm; voxel size = 1 × 1 × 1 mm^3, out-of-plane SENSE parallel reduction factor = 1.5, sagittal orientation).

2.7. MRI analysis

MRI analysis was performed at the Neuroimaging Research Unit, IRCCS San Raffaele Scientific Institute, Milan, Italy, by experienced observers, blinded to subjects' identity. The presence of vascular abnormalities, including WM hyperintensities and lacunes, was checked on DE images.

2.7.1. Cortical thickness measurement

Cortical reconstruction and estimation of cortical thickness were performed on the 3D T1-weighted TFE images using the FreeSurfer image analysis suite, version 5.3 (http://surfer.nmr.mgh.harvard.edu/) (Fischl and Dale, 2000). On all 3D TFE images, the contrast between GM and white matter (WM) was enhanced by nulling out all image values below the mean intensity of the cerebrospinal fluid (CSF), and by performing a rescaling of all image intensities above threshold to the new null value. After registration to Talairach space and intensity normalization, the process involved an automatic skull stripping, which removes extra-cerebral structures, cerebellum and brainstem, by using a hybrid method combining watershed algorithms and deformable surface models. Images were carefully checked for skull stripping errors. Then, images were segmented into GM, WM, and CSF, cerebral hemispheres were separated, and subcortical structures divided from cortical components. The WM/GM boundary was tessellated and the surface was deformed following intensity gradients to optimally place WM/GM and GM/CSF borders, thus obtaining the WM and pial surfaces (Dale et al., 1999). Afterwards, surface inflation and registration to a spherical atlas were performed (Dale et al., 1999) and the cerebral cortex parcellated into 34 regions of interest (ROIs) per hemisphere, based on gyral and sulcal structures (Desikan et al., 2006). Finally, cortical thickness was estimated as the average shortest distance between the WM boundary and the pial surface. Surface maps were generated following registration of all subjects' cortical reconstructions to a common average surface and then smoothed using a surface-based Gaussian kernel of 10 mm full width half-maximum. To evaluate longitudinal cortical changes in PD patients, the four serial 3D TFE images of each subject were processed with the Freesurfer longitudinal stream (Reuter et al., 2010). Specifically, an unbiased within-subject template space and image was created from the four scans using a robust, inverse consistent registration. Several processing steps (including skull stripping, Talairach transforms, atlas registration, as well as spherical surface maps and parcellations) were then initialized on the four scans, with common information from the within-subject template. This allowed to create surface maps of the four timepoints with a significantly increased reliability and statistical power compared to those produced by the cross-sectional Freesurfer pipeline (Reuter et al., 2010). Individual surface maps were registered to a common average surface and then smoothed using a Gaussian kernel of 10 mm full width half-maximum.

2.7.2. Deep GM volumes

FMRIB's Integrated Registration and Segmentation Tool (FIRST) in FSL (http://www.fmrib.ox.ac.uk/fsl/first/index.html) was applied to

Table 1
Demographic characteristics at study entry in healthy controls (HC), mild PD, mild motor-predominant PD, mild-diffuse PD and moderate-to-severe PD patients.

Variables	HC	Mild PD	Mild motor-predominant PD	Mild-diffuse PD	Moderate-to-severe PD	p: Mild PD *vs* HC	p: Mild motor-predominant PD *vs* HC	p: Mild-diffuse PD *vs* HC	p: Moderate-to-severe PD *vs* HC	p: Mild motor-predominant PD *vs* Mild-diffuse PD	p: Moderate-to-severe PD *vs* Mild PD
Age at MRI [years]	61.8 ± 8.9 (46.1–77.7)	60.3 ± 8.0 (39.4–75.9)	58.0 ± 8.8 (39.37–75.87)	62.5 ± 6.6 (42.28–74.74)	63.3 ± 7.6 (44.9–83.0)	0.47	0.10	0.53	0.45	0.07	0.19
Sex [Men/ Women]	29 (48.3)/ 31 (51.7)	49 (56.3)/ 38 (43.7)	12 (27.9)/ 31 (72.1)	37 (84.1)/ 7 (15.9)	42 (62.7)/ 25 (37.3)	0.51	**0.04**	**< 0.001**	0.33	**< 0.001**	0.51
Education [years]	13.5 ± 2.6 (8.0–16.0)	13.2 ± 2.5 (7.0–20.0)	12.8 ± 2.4 (7.0–17.0)	13.6 ± 2.6 (8.0–20.0)	11.4 ± 2.4 (4.0–16.0)	0.47	0.26	0.98	**< 0.001**	0.26	**< 0.001**
Handedness [Right/Left/ Both]	46 (92)/ 4 (8)/ 0 (0)	84 (97.7)/ 2 (2.3)/ 0 (0)	41 (97.6) 1 (2.4) 0 (0)	43 (97.7) 1 (2.3) 0 (0)	60 (92.3)/ 4 (6.1)/ 1 (1.5)	0.33	0.56	0.56	0.85	1.00	0.33
Age at onset [years]	–	58.3 ± 8.1 (38.0–74.0)	55.4 ± 8.8 (38.0–73.0)	61.19 ± 6.30 (43.0–74.0)	54.4 ± 7.9 (41.0–76.0)	–	–	–	–	**< 0.001**	**< 0.001**
PD duration [years]	–	1.9 ± 1.8 (0.0–10.3)	2.6 ± 2.1 (0.1–10.3)	1.3 ± 1.2 (0.0–5.0)	8.8 ± 4.8 (0.9–23.9)	–	–	–	–	**< 0.001**	**< 0.001**
Family history [No/Yes]	–	69 (79.3)/ 18 (20.7)	34 (79.1)/ 9 (20.9)	35 (79.5)/ 9 (20.4)	61 (91.0)/ 6 (9.0)	–	–	–	–	1.00	0.07
Side of onset [Right/Left/ Both]	–	50 (57.5)/ 36 (41.4)/ 1 (1.1)	25 (58.1)/ 18 (41.9)/ 0 (0)	25 (56.8)/ 18 (40.9)/ 1 (2.3)	47 (70.1)/ 18 (26.9)/ 2 (3.0)	–	–	–	–	1.00	0.10

Values are reported as mean ± standard deviation (range) or absolute and percentage frequency (%) for continuous and categorical variables, respectively. Differences between groups at baseline were assessed using one-way ANOVA (for continuous demographic and general clinical variables). P-values were adjusted for multiple comparisons controlling the False Discovery Rate (FDR) at level 0.05 using Benjamini-Hochberg step-up procedure. Values in bold indicate statistically significant results. ***Abbreviations:*** *HC = healthy controls; PD = Parkinson's disease.*

Table 2
Clinical characteristics and changes over time in mild PD and moderate-to-severe PD patients.

Variables	Mild PD	Moderate-to-severe PD	p: Moderate-to-severe PD *vs* Mild PD	Annualized mean rate of change (i.e. linear trend) in Mild PD	Annualized mean rate of change (i.e. linear trend) in Moderate-to-severe PD	p for linear trend Mild PD	p for linear trend Moderate-to-severe PD	p for differential trend Mild PD *vs* Moderate-to-severe PD
Levodopa equivalent dose [mg]	250.3 ± 241.3 (0.0–1280.0)	853.2 ± 337.8 (0.0–1930.0)	**< 0.001**	162.4%	52.9%	**< 0.001**	**< 0.001**	**< 0.001**
Clinical motor variables								
Hoehn & Yahr	1.1 ± 0.3 (1.0–2.5)	2.5 ± 0.6 (1.0–4.0)	**< 0.001**	7.2%	2.4%	**< 0.001**	**< 0.001**	**< 0.001**
UPDRS Total	28.2 ± 10.8 (7.0–66.0)	62.4 ± 15.9 (17.0–103.0)	**< 0.001**	116.5%	41.5%	**< 0.001**	**< 0.001**	**< 0.001**
UPDRS II Total	5.8 ± 3.5 (0.0–19.0)	13.63 ± 4.42 (2.0–23.0)	**< 0.001**	157.9%	70.2%	**< 0.001**	**< 0.001**	**< 0.001**
UPDRS III Total	17.4 ± 7. (5.0–52.0)	43.1 ± 11.1 (13.0–76.0)	**< 0.001**	105%	28.0%	**< 0.001**	**< 0.001**	**< 0.001**
UPDRS III Axial	1.8 ± 1.1 (0.0–5.0)	5.2 ± 1.9 (1.0–10.0)	**< 0.001**	125%	64.7%	**< 0.001**	**< 0.001**	**0.02**
UPDRS III Bradykinesia	7.8 ± 4.2 (3.0–27.0)	22.5 ± 5.6 (6.0–32.0)	**< 0.001**	140.2%	22.3%	**< 0.001**	**< 0.001**	**< 0.001**
UPDRS III Rigidity	3.0 ± 2.0 (0.0–13.0)	9.6 ± 2.7 (3.0–14.0)	**< 0.001**	99.1%	21.8%	**< 0.001**	**0.002**	**< 0.001**
UPDRS IV Total	0.1 ± 0.4 (0.0–3.0)	2.6 ± 2.1 (0.0–9.0)	**< 0.001**	1309.8%	41.7%	**< 0.001**	**0.02**	**< 0.001**
***UPDRS IV Dyskinesia* [No/Yes]**	85 (97.7)/ 2 (2.3)	27 (40.3)/ 40 (59.7)	**< 0.001**	–	–	–	–	–
***UPDRS IV Fluctuation* [No/Yes]**	85 (97.7)/ 2 (2.3)	23 (34.3)/ 44 (65.7)	**< 0.001**	–	–	–	–	–
FoG-Q	0.8 ± 1.1 (0.0–5.0)	5.6 ± 4.4 (0.0–18.0)	**< 0.001**	304.1%	20.3%	**< 0.001**	0.08	**< 0.001**
Clinical non-motor variables								
RBDSQ	2.5 ± 2.6 (0–11)	4.3 ± 2.9 (1–12)	**< 0.001**	–	–	–	–	–
UPDRS I Total	5.0 ± 3.75 (0.0–16.0)	3.0 ± 2.5 (0.0–12.0)	**< 0.001**	87.3%	95.8%	**< 0.001**	**< 0.001**	0.146
***UPDRS I Hallucinations and psychosis* [No/Yes]**	81 (93.1)/ 6 (6.9)	45 (67.2)/ 22 (32.8)	**< 0.001**	–	–	–	–	–
***NMS-Q Gastrointestinal symptoms* [No/Yes]**	38 (43.7)/ 49 (56.3)	9 (13.4)/ 58 (86.6)	**< 0.001**	–	–	–	–	–
***NMS-Q Urinary symptoms* [No/Yes]**	44 (50.6)/ 43 (49.4)	10 (14.9)/ 57 (85.1)	**< 0.001**	–	–	–	–	–
***NMS-Q Olfactory dysfunction* [No/Yes]**	67 (77.0)/ 20 (23.0)	47 (70.1)/ 20 (29.8)	0.359	–	–	–	–	–
***NMS-Q Sexual dysfunction* [No/Yes]**	57 (65.5)/ 30 (34.5)	20 (29.8)/ 47 (70.1)	**< 0.001**	–	–	–	–	–
***NMS-Q Orthostatic symptoms* [No/Yes]**	74 (86.0)/ 12 (13.9)	35 (52.2)/ 32 (47.8)	**< 0.001**	–	–	–	–	–

Values are reported as mean ± standard deviation (range) or absolute and percentage frequency (%) for continuous and categorical variables, respectively. Differences between PD groups at baseline were assessed using one-way ANOVA (for continuous general clinical variables), Poisson regression which accounted for overdispersion (for continuous clinical motor and non-motor variables), Fisher test (for all categorical variables). Annualized mean rate of changes (%) was obtained (for continuous variables only) as the percentage difference between the variable mean at the end of follow-up (estimated by means of the regression slope found in a longitudinal model which included time as continuous variable) and the estimated variable mean at baseline. P-values were adjusted for multiple comparisons controlling the False Discovery Rate (FDR) at level 0.05 using Benjamini-Hochberg step-up procedure. Values in bold indicate statistically significant results. ***Abbreviations:*** *FoG-Q = freezing of gait questionnaire; HC = healthy controls; NMS-Q = Non-Motor Symptoms Questionnaire; PD = Parkinson's disease; RBDSQ = REM Sleep Behaviour Disorder Screening Questionnaire; UPDRS = Unified Parkinson's Disease Rating Scale.*

TFE images of each subject at each visit and used to automatically segment GM regions, i.e., caudate, pallidum, putamen, thalamus and nucleus accumbens, amygdala and hippocampus, bilaterally. Mean GM volumes were calculated and multiplied by the normalization factor derived from SIENAx to correct for subject head size (http://www.fmrib.ox.ac.uk/fsl/sienax/index.html).

2.8. Statistical analysis

2.8.1. Demographic, clinical and cognitive data

Demographic and clinical general data were compared between groups using ANOVA models or Fisher exact test. For clinical motor, non-motor and cognitive variables, Poisson regressions, which accounted for overdispersion, were performed. Changes in continuous variables over time were assessed by the annualized mean rate of change (%), calculated from the regression slope of a generalized linear model for longitudinal data (using Poisson as link function) for clinical continuous variables, using time as continuous variable. Test for linear trend (associated with the annualized mean rate) was estimated in PD groups and group-by-time interaction was assessed to evaluate longitudinal between-group differences. P values were adjusted for multiple comparisons controlling the False Discovery Rate (FDR) at level 0.05 using Benjamini-Hochberg step-up procedure. Two-sided p value < 0.05 was considered for statistical significance. Analyses were performed using SAS (Release 9.4, SAS Institute, Cary, NC, USA).

2.8.2. Baseline MRI findings

A cross-sectional vertex-by-vertex analysis was performed to assess differences of cortical thickness between groups at baseline, using a general linear model in FreeSurfer adjusting for age. Maps showing baseline comparisons were obtained by thresholding the t-statistic at $p < 0.05$, FDR-corrected for multiple comparisons. The mean cortical thickness of 34 ROIs per hemisphere (Desikan et al., 2006) and the mean GM volumes were compared between groups using ANOVA models, FDR-corrected for multiple comparisons at level of 0.05 adjusting for age (SAS).

2.8.3. Longitudinal MRI findings

Longitudinal changes of cortical thickness occurring within PD patient groups (mild PD; moderate-to-severe PD; mild-diffuse PD; mild motor-predominant PD) and between groups over the four timepoints (group × time interaction: mild PD *vs* moderate-to-severe PD; mild-diffuse PD *vs* mild motor-predominant PD) were assessed using Linear Mixed Effects Models in Freesurfer (Bernal-Rusiel et al., 2013) adjusting for age, LEDD change over time, and time interval between baseline and follow-up scans. Maps showing the rate of cortical thinning over time were obtained by thresholding the t-statistic at $p < 0.05$, FDR-corrected for multiple comparisons.

Changes over time in the mean cortical thickness of the 34 ROIs and the mean GM volumes were assessed by the annualized mean rate of change (%), calculated from the regression slope of ANOVA model for longitudinal data, using time as continuous variable. Test for linear trend (associated with the annualized mean rate) was estimated in PD groups and group-by-time interaction was assessed to evaluate longitudinal between-group differences (mild PD *vs* moderate-to-severe PD; mild-diffuse PD *vs* mild motor-predominant PD). Such models were adjusted for age and LEDD (treated as time-varying covariate). P values were adjusted for multiple comparisons controlling the FDR at level 0.05 using Benjamini-Hochberg step-up procedure. Two-sided p value < 0.05 was considered for statistical significance (SAS).

2.8.4. MRI prediction models of clinical evolution

In each PD group, linear regression models assessed the associations of baseline MRI metrics (which were found to be significantly different between groups) and baseline MRI metrics + 1-year change with the four GCOs. Stepwise model selection procedure was applied to candidate baseline MRI metrics and 1-year changes chosen a priori on the basis of MRI variables that were significantly different between patients and controls at baseline and that showed significant annualized mean rate of change in each group (significance level for entry and staying into the model: $p = 0.10$). Each GCO was considered as the dependent variable into each model, which also included age, baseline LEDD, and individual follow-up duration (independent variables). R^2 goodness of fit statistic was estimated for each model at issue, for each PD subtype separately. Two-sided p value < 0.05 was considered for statistical significance. Analyses were performed using SAS.

3. Results

3.1. Baseline clinical findings

Two PD clusters were identified at baseline: 87 patients were classified as mild PD and 67 as moderate-to-severe PD, with the latter group having lower education, earlier PD onset, longer PD duration, more severe motor signs and symptoms, more severe and frequent non-motor manifestations, more severe cognitive dysfunctions and higher LEDD (demographic variables are presented in Table 1; general clinical variables in Table 2; and cognitive variables in Supplemental table 1). Within the mild PD cluster, two clinical subtypes were further identified: mild motor-predominant ($N = 43$) and mild-diffuse ($N = 44$), with the latter group being slightly older, more frequently male, and having later PD onset, shorter PD duration, more frequent non-motor manifestations (i.e., REM sleep behaviour disorders and urinary dysfunction) and greater global cognitive dysfunction and memory deficits (demographic variables are presented in Table 1; general clinical variables in Table 3; and cognitive variables in Supplemental table 2).

3.2. Longitudinal clinical findings

Clinical and cognitive changes in PD subtypes are reported in Tables 2 and 3, Supplemental Tables 1 and 2. Over time, mild PD compared to moderate-to-severe PD patients showed greater worsening of motor variables, while moderate-to-severe patients showed greater worsening of cognitive abilities. Both mild and moderate-to-severe PD groups showed a significant worsening of UPDRS I, depression and apathy scores, without differences between groups over time. Only the moderate-to-severe group showed anxiety worsening over the follow-up. Both mild and moderate-to-severe PD groups showed an increased frequency of fluctuations (mild FDR-corrected $p < 0.001$; moderate-to-severe FDR-corrected $p = 0.01$) and dyskinesia (mild FDR-corrected $p = 0.02$; moderate-to-severe FDR-corrected $p = 0.01$) over time, with mild PD showing also an increased frequency of REM sleep behavior disorders (FDR-corrected $p = 0.001$), orthostatic symptoms (FDR-corrected $p = 0.03$) and hallucinations (FDR-corrected $p = 0.04$).

Within the mild PD group, both mild-diffuse and motor-predominant PD clusters worsened in all motor variables and UPDRS I, without any significant difference between groups in time (Table 3). Mild motor-predominant cases had an increased frequency of orthostatic symptoms (FDR-corrected $p = 0.04$), dyskinesia (FDR-corrected $p = 0.03$), fluctuations (FDR-corrected $p = 0.002$) and REM sleep behavior disorders (FDR-corrected $p = 0.02$), while mild-diffuse PD cases showed increased frequency of fluctuations (FDR-corrected $p = 0.005$). Mild-diffuse PD patients showed significant worsening of executive functions, attention and visuospatial abilities, with no difference between groups over time. Both mild-diffuse and mild motor-predominant PD groups showed worsening of depression and apathy, with no difference between groups over time.

3.3. Baseline MRI findings

3.3.1. Cortical thickness

A widespread pattern of bilateral cortical thinning involving frontal,

Table 3
Clinical characteristics and changes over time in mild motor-predominant PD and mild-diffuse PD patients.

Variables	Mild motor-predominant PD	Mild-diffuse PD	p: Mild motor-predominant PD *vs* Mild-diffuse PD	Annualized mean rate of change (i.e. linear trend) in Mild motor-predominant PD	Annualized mean rate of change (i.e. linear trend) in Mild-diffuse PD	p for linear trend Mild motor-predominant PD	p for linear trend Mild-diffuse PD	p for differential trend Mild motor-predominant PD *vs* Mild-diffuse PD
Levodopa equivalent dose [mg]	299.5 ± 251.4 (0.0–1280.0)	202.3 ± 223.6 (0.0–970.0)	0.07	127.2%	207.4%	< **0.001**	< **0.001**	0.16
Clinical motor variables								
Hoehn & Yahr	1.1 ± 0.2 (1.0–2.0)	1.1 ± 0.3 (1.0–2.5)	0.97	109.8%	90.8%	< **0.001**	< **0.001**	0.37
UPDRS Total	27.4 ± 10.0 (7.0–58.0)	29.0 ± 11.6 (9.0–66.0)	0.49	115.9%	117.3%	< **0.001**	< **0.001**	0.96
UPDRS II Total	5.5 ± 3.1 (0.0–11.0)	6.1 ± 3.9 (0.0–19.0)	0.46	163.3%	153.8%	< **0.001**	< **0.001**	0.84
UPDRS III Total	17.4 ± 7.7 (5.0–50.0)	17.32 ± 7.69 (7.0–52.0)	0.94	97.2%	112.3%	< **0.001**	< **0.001**	0.62
UPDRS III Axial	1.9 ± 1.1 (0.0–4.0)	1.7 ± 1.1 (0.0–5.0)	0.36	115.1%	135.0%	< **0.001**	< **0.001**	0.72
UPDRS III Bradykinesia	8.2 ± 4.3 (3.0–27.0)	7.4 ± 4.1 (3.0–24.0)	0.33	130.7%	150.5%	< **0.001**	< **0.001**	0.95
UPDRS III Rigidity	3.2 ± 2.9 (0.0–13.0)	2.9 ± 1.8 (0.0–9.0)	0.45	114.2%	84.4%	< **0.001**	< **0.001**	0.52
UPDRS IV Total	0.1 ± 0.5 (0.0–3.0)	0.05 ± 0.3 (0.0–2.0)	0.23	1282.9%	1519.0%	< **0.001**	**0.002**	0.86
***UPDRS IV Dyskinesia* [No/Yes]**	41 (95.3)/ 2 (4.6)	44 (100.0)/ 0 (0.0)	0.24	–	–	**–**	**–**	–
***UPDRS IV Fluctuation* [No/Yes]**	42 (97.7)/ 1 (2.3)	43 (97.7)/ 1 (2.3)	1.00	–	–	**–**	**–**	–
FoG-Q	0.9 ± 1.3 (0.0–5.0)	0.6 ± 0.9 (0.0–4.0)	0.21	289.5%	330.6%	< **0.001**	< **0.001**	0.80
Clinical non-motor variables								
RBDSQ	2.0 ± 2.0 (0.0–8.0)	3.0 ± 3.0 (1.0–11.0)	**0.04**	–	–	–	–	–
UPDRS I Total	4.4 ± 3.1 (0.0–11.0)	5.6 ± 4.2 (0.0–16.0)	0.15	99.8%	76.1%	< **0.001**	**0.001**	0.62
***UPDRS I Hallucinations and psychosis* [No/Yes]**	40 (93.0)/ 3 (7.0)	41 (93.2)/ 3 (6.8)	1.00	–	–	–	–	–
***NMS-Q Gastrointestinal symptoms* [No/Yes]**	20 (46.5)/ 23 (53.5)	18 (40.9)/ 26 (59.1)	0.69	–	–	–	–	–
***NMS-Q Urinary symptoms* [No/Yes]**	31 (72.1)/ 12 (27.9)	13 (29.5)/ 31 (70.4)	< **0.001**	–	–	–	–	–
***NMS-Q Olfactory dysfunction* [No/Yes]**	34 (79.1)/ 9 (20.9)	33 (75)/ 11 (25)	0.80	–	–	–	–	–
***NMS-Q Sexual dysfunction* [No/Yes]**	30 (69.8)/ 13 (30.2)	27 (61.4)/ 17 (38.6)	0.50	–	–	–	–	–
***NMS-Q Orthostatic symptoms* [No/Yes]**	37 (88.1)/ 5 (11.9)	37 (84.1)/ 7 (15.9)	0.76	–	–	–	–	–

Values are reported as mean ± standard deviation (range) or absolute and percentage frequency (%) for continuous and categorical variables, respectively. Differences between PD groups at baseline were assessed using one-way ANOVA (for continuous general clinical variables), Poisson regression which accounted for overdispersion (for continuous clinical motor and non-motor variables), Fisher test (for all categorical variables). Annualized mean rate of changes (%) was obtained (for continuous variables only) as the percentage difference between the variable mean at the end of follow-up (estimated by means of the regression slope found in a longitudinal model which included time as continuous variable) and the estimated variable mean at baseline. P-values were adjusted for multiple comparisons controlling the False Discovery Rate (FDR) at level 0.05 using Benjamini-Hochberg step-up procedure. Values in bold indicate statistically significant results.
Abbreviations: *FoG-Q = freezing of gait questionnaire; HC = healthy controls; NMS-Q = Non-Motor Symptoms Questionnaire; PD = Parkinson's disease; RBDSQ = REM Sleep Behaviour Disorder Screening Questionnaire; UPDRS = Unified Parkinson's Disease Rating Scale.*

parietal, temporal and occipital lobes was found in moderate-to-severe patients relative to healthy controls and mild PD patients (Fig. 2A). No significant cortical thickness differences were found in mild PD relative to healthy controls (Fig. 2B). A diffuse pattern of cortical thinning was observed in moderate-to-severe relative to mild motor-predominant PD patients (Fig. 3A). When compared to mild-diffuse PD, moderate-to-severe patients showed few spots of cortical thinning in parietal and occipital lobes bilaterally, right temporo-parietal junction and rostral middle frontal gyrus (Fig. 3B). No significant cortical thickness differences were found when mild motor-predominant and mild-diffuse PD

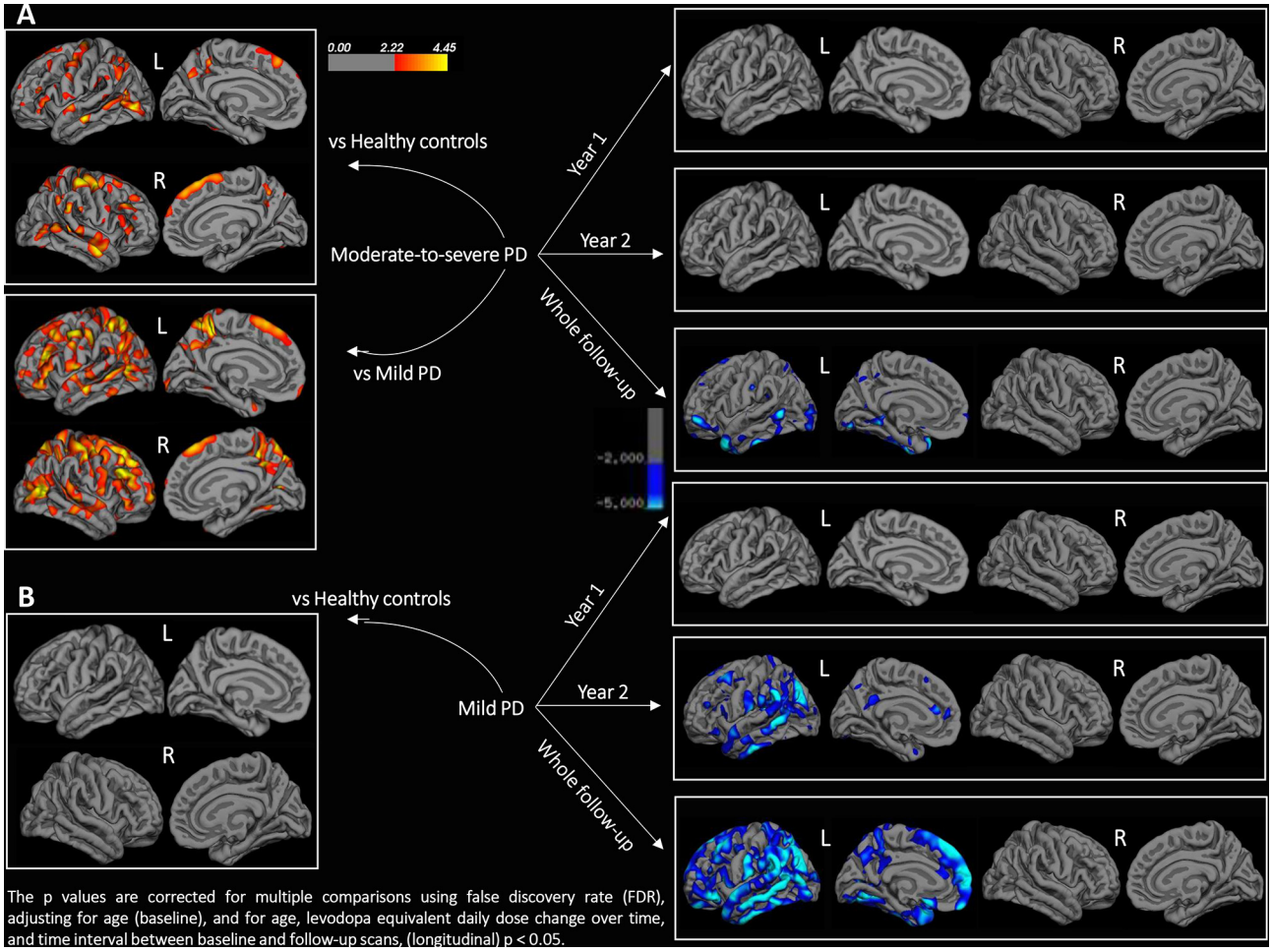

Fig. 2. (On the left) Cortical thinning patterns at baseline in A) moderate-to-severe PD patients compared to healthy controls and mild PD, and in B) mild PD patients compared to healthy controls. (On the right) Cortical thinning over year 1, year 2 and whole follow-up in A) moderate-to-severe PD patients and in (B) mild PD patients. The p values are corrected for multiple comparisons using false discovery rate (FDR), adjusting for age (baseline) and for age, levodopa equivalent daily dose change over time, and time interval between baseline and follow-up scans (longitudinal), $p < 0.05$. Color bar represents t-values. *L = left; R = right.*

patients were compared with healthy controls and each other (Fig. 4A and B). Results were significant at FDR-corrected $p < 0.05$.

3.3.2. GM volumes

Results are shown in Table 4. At baseline, moderate-to-severe PD patients showed a reduced volume of bilateral caudate nuclei and right hippocampus relative to healthy controls and mild PD patients. Mild-diffuse PD patients showed a reduced volume of the right hippocampus relative to mild motor-predominant PD subjects. Results were significant at FDR-corrected $p < 0.05$.

3.4. Longitudinal MRI changes

3.4.1. Cortical thickness over one and two years of follow-up

Over one year of follow-up, only mild motor-predominant PD patients showed cortical atrophy (Fig. 4A); no longitudinal atrophy changes were observed in the other PD groups (Fig. 2A, 2B and 4B). In the comparison between groups over one year of follow-up, only mild motor-predominant relative to mild-diffuse PD patients showed greater atrophy accumulation in the left temporal lobe (group × time interaction; Fig. 4A). Results were significant at FDR-corrected $p < 0.05$.

Over two years of follow-up, mild PD patients showed widespread progressive cortical thinning in the left hemisphere (mainly in the temporal and parietal lobes) (Fig. 2B), while moderate-to-severe PD did not show cortical atrophy (Fig. 2A). Cortical thickness changes over two years of follow-up were not significantly different between mild and moderate-to-severe PD patients (group × time interaction).

When mild PD groups were analyzed separately, mild motor-predominant PD cases showed cortical thinning in few regions of the left hemisphere (Fig. 4A), while mild-diffuse patients did not show any cortical atrophy over two years of follow-up (Fig. 4B). However, the direct comparison between mild motor-predominant and mild-diffuse PD groups did not show any significant difference in cortical thickness changes over two years (group × time interaction). Results were significant at FDR-corrected $p < 0.05$.

3.4.2. Cortical thickness over the whole follow-up

Over the whole follow-up, both mild and moderate-to-severe PD clusters showed progressive cortical thinning. A widespread whole brain cortical thinning was evident in mild PD patients (Fig. 2B), while less distributed atrophy progression was observed in moderate-to-severe PD patients (mainly in the left temporal lobe, orbitofrontal regions and occipital lobe; Fig. 2A). The direct comparison between mild and moderate-to-severe PD patients did not show any significant difference in cortical thickness changes over the whole follow-up (group × time interaction). Within the mild PD group, mild motor-predominant PD patients showed cortical thinning accumulation in few regions of the temporal, occipital and medial frontal lobes (Fig. 4A), while mild-diffuse PD cases showed the most widespread cortical thinning (Fig. 4B). Cortical thickness changes were not significantly different between mild motor-predominant and mild-diffuse PD patients over the whole follow-up (group × time interaction). Results were significant at FDR-

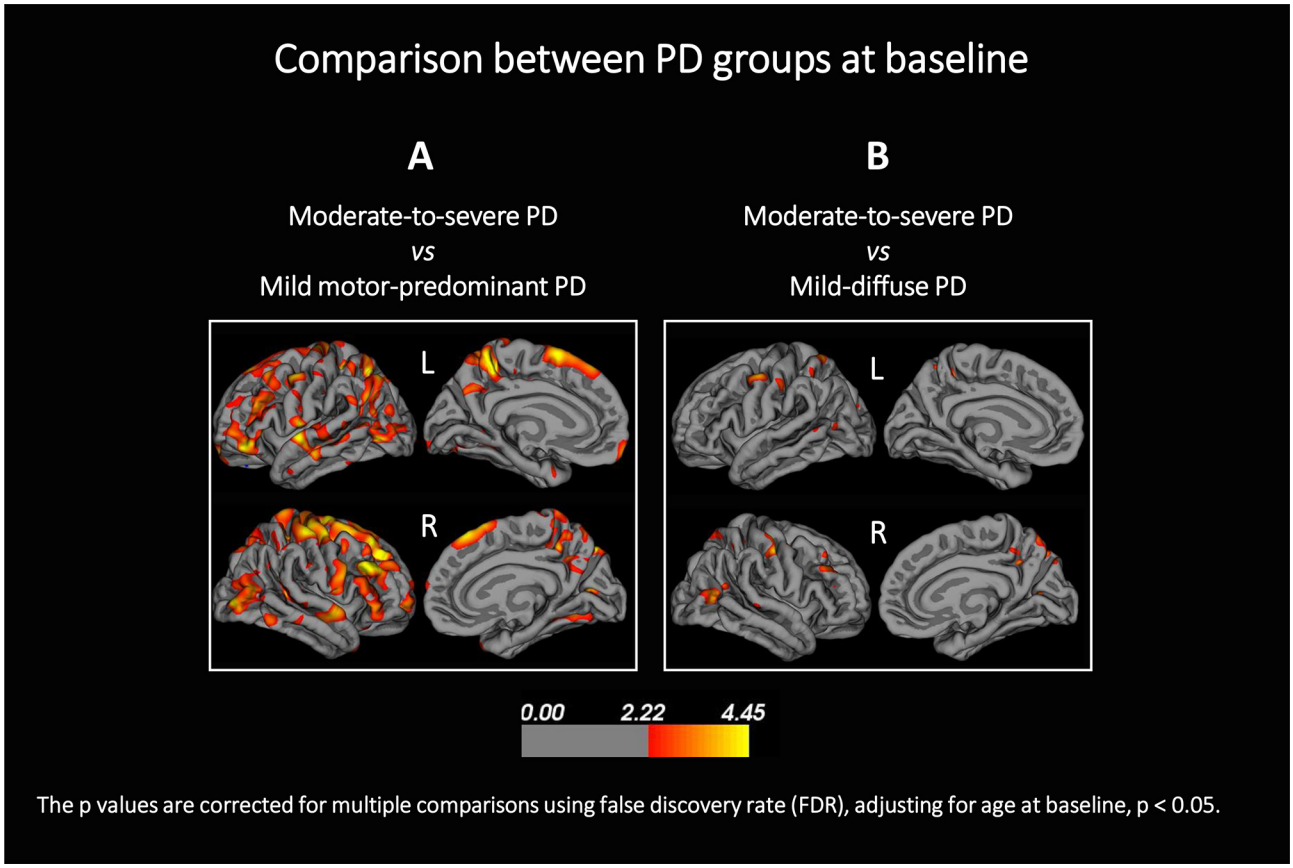

Fig. 3. Cortical thinning at baseline between moderate-to-severe PD patients and (A) mild motor-predominant PD patients, and (B) mild-diffuse PD patients. The p values are corrected for multiple comparisons using false discovery rate (FDR) adjusting for age, $p < 0.05$. Color bar represents t-values. *L = left; R = right.*

corrected $p < 0.05$.

3.4.3. GM volumes over one and two years of follow-up

Mild and moderate-to-severe PD patients did not show any significant change in GM volumes over one and two years. When mild cases were clustered into two groups, mild-motor predominant PD patients showed a significant atrophy of the left pallidum over one year (FDR-corrected $p = 0.04$, annualized mean rate of change = -2.2%). GM volumes changes were not significantly different between none of the PD groups over one and two years of follow-up (group × time interaction).

3.4.4. GM volumes over the whole follow-up

Mild and moderate-to-severe PD patients did not show any significant change in GM volumes over time. When mild cases were clustered into two groups, mild-diffuse PD patients showed a significant atrophy of the left hippocampus (FDR-corrected $p = 0.01$). GM volumes changes were not significantly different between none of the PD groups over the whole follow-up (group × time interaction). Results are shown in Table 4.

3.5. The effect of structural brain changes on clinical PD progression

Table 5 summarizes the ability of cortical thickness alterations at baseline and at baseline + 1-year change to predict clinical evolution over time in PD groups. The longitudinal changes over the whole follow-up of the 34 ROI mean cortical thickness values in PD groups were used to select variables for prediction models and are shown in Supplemental Table 3.

4. Discussion

Investigating biomarkers to predict progression of PD is of high priority. Longitudinal MRI studies have the potential to provide a characterization of disease progression related to clinical manifestations and might guide our understanding of the underlying neurodegenerative processes. Using serial structural MRI data from a large sample of PD patients, we showed that cortical and subcortical GM have different patterns and rates of atrophy according to disease stage and clinical subtype. Specifically, this study showed that cortical thickness analysis has a high sensitivity to progressive brain structural damage accumulation in PD, especially in the mild phase of the disease. A key finding was that baseline and 1-year cortical thinning was associated with long-term progression of motor, cognitive, non-motor and mood symptoms.

A severe brain atrophy was demonstrated in the basal ganglia, sensorimotor areas, frontal and posterior brain regions, particularly in bilateral occipital, temporal and parietal lobes, in moderate-to-severe PD patients at baseline. This pattern suggests a widespread GM modification in PD patients with high severity of motor and non-motor symptoms, in agreement with previous MRI results (Agosta et al., 2013b; Lewis et al., 2016; Melzer et al., 2012; Sterling et al., 2016) and pathological studies (Braak et al., 2006). Importantly, longitudinal analysis showed that no cortical thinning is present over one and two years of follow-up in moderate-to-severe patients, but brain atrophy increases over longer periods (three to four years) in these subjects, involving mainly in temporo-occipital and ventral frontal regions. Even if we did not have longitudinal MRI data from healthy controls, our findings are in line with previous studies comparing PD subjects with healthy controls over time (Lewis et al., 2016; Mak et al., 2015; Hanganu et al., 2013; Melzer et al., 2012; Ibarretxe-Bilbao et al., 2012).

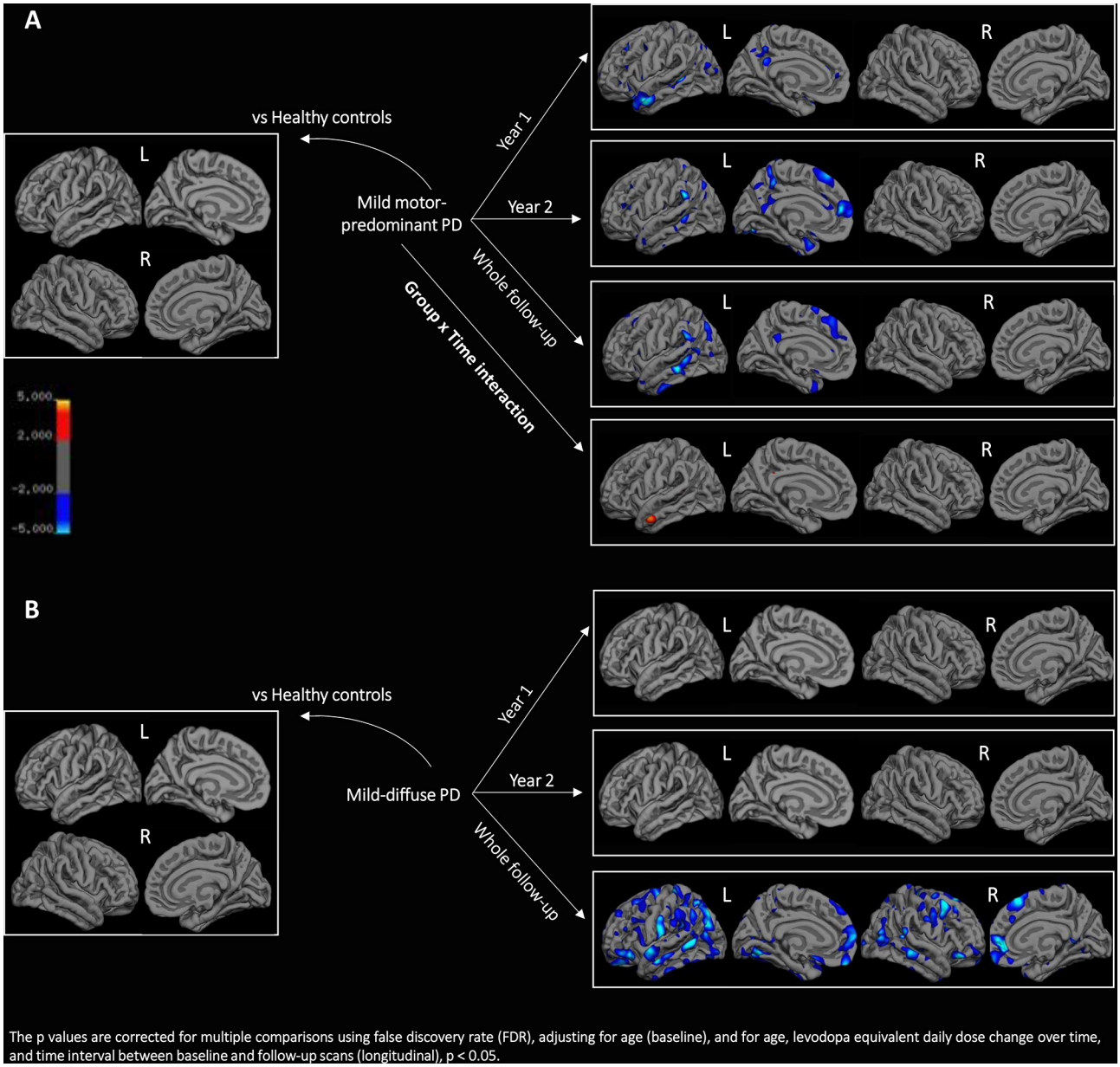

Fig. 4. (On the left) Cortical thinning patterns at baseline in A) mild motor-predominant PD patients compared to healthy controls and in B) mild-diffuse PD patients compared to healthy controls. (On the right) Cortical thinning over year 1, year 2, and whole follow-up in A) mild motor-predominant PD patients and in (B) mild-diffuse PD patients and group × time interaction between them (A). The p values are corrected for multiple comparisons using false discovery rate (FDR), adjusting for age (baseline) and for age, levodopa equivalent daily dose change over time, and time interval between baseline and follow-up scans (longitudinal), $p < 0.05$. Color bar represents t-values. *L = left; R = right.*

The specific damage of associative frontal, parietal, temporal and occipital regions in moderate-to-severe PD patients has been related with a spectrum of cognitive deficits (Camicioli et al., 2011; Garcia-Diaz et al., 2018; Gorges et al., 2020; Hanganu et al., 2013; Lewis et al., 2016; Mak et al., 2015). A recent longitudinal study that compared PD patients and controls over five years of follow-up showed widespread cortical (fronto-temporal and parieto-occipital) thinning in PD patients with normal cognition, more pronounced damage in patients with cognitive impairment, and a correlation between cortical thinning in the caudal anterior cingulate and lower cognitive performance in patients that convert to cognitive impairment or dementia (Gorges et al., 2020). Non-motor PD manifestations such as depression (Hanganu et al., 2017), hyposmia (Baba et al., 2012), and hallucinations (Ibarretxe-Bilbao et al., 2010) were previously associated with a progressive loss of brain volume.

The most interesting findings were observed in the mild PD clusters. Screening patients for motor, cognitive and other non-motor features at baseline, our study identified a mild-diffuse PD cluster characterized by an initial aggressive disease and greater brain atrophy and cognitive dysfunction accumulation over time. These patients were initially older, more frequently male and had later PD onset, shorter PD duration, more frequent non-motor manifestations and more severe global cognitive dysfunction and memory deficits relative to mild motor-predominant cases. Over time, both mild subtypes showed motor and non-motor clinical evolution. However, mild-diffuse patients were more likely to have significant worsening of executive functions, attention and visuospatial abilities. Old age at onset and non-motor status are well-known critical determinants of PD prognosis (Fereshtehnejad et al., 2017; van Rooden et al., 2010). Accordingly, MRI data pointed toward a relatively early diffuse neurodegenerative process in this group.

Table 4
Grey matter volumes at study entry in healthy controls (HC), mild PD, mild motor-predominant PD, mild-diffuse PD and moderate-to-severe PD patients and changes over time in PD patients.

Variables	Side	HC	Mild PD	Moderate-to-severe PD	p: Mild PD *vs* HC	p: Moderate-to-severe PD *vs* HC	p: Moderate-to-severe PD *vs* Mild PD	Annualized mean rate of change (i.e. linear trend) in Mild PD	Annualized mean rate of change (i.e. linear trend) in Moderate-to-severe PD	p for linear trend Mild PD	p for linear trend Moderate-to-severe PD	p for differential trend Mild PD *vs* Moderate-to-severe PD
Amygdala	L	1791.0 ± 275.2 (1039.5–2397.2)	1845.7 ± 268.1 (969.3–2507.3)	1822.9 ± 299.9 (1143.7–2607.2)	0.68	0.68	0.68	−1.3%	0.9%	0.66	0.79	0.58
	R	1846.3 ± 317.2 (858.1–2355.7)	1810.9 ± 341.0 (608.1–2685.8)	1808.5 ± 333.5 (936.8–2518.1)	0.83	0.83	0.83	−1.0%	2.8%	0.79	0.50	0.45
Caudate	L	4298.6 ± 495.0 (2948.7–5576.8)	4305.0 ± 477.5 (3258.8–5427.3)	3972.7 ± 372.3 (3072.0–4676.1)	0.81	**< 0.001**	**< 0.001**	−0.7%	−0.3%	0.69	0.89	0.86
	R	4523.0 ± 426.6 (515.5–5783.4)	4477.0 ± 543.7 (2355.0–5618.9)	4143.1 ± 458.0 (2974.4–5434.2)	0.40	**< 0.001**	**< 0.001**	−1.0%	0.5%	0.59	0.81	0.55
Hippocampus	L	4922.6 ± 507.4 (3806.4–6175.1)	4911.0 ± 474.4 (3875.4–6120.9)	4885.1 ± 651.1 (3214.3–6166.0)	0.91	0.91	0.91	−2.7%	−2.3%	0.11	0.21	0.90
	R	5120.9 ± 591.9 (3952.6–7879.1)	5147.1 ± 500.9 (2791.1–6123.4)	5085.1 ± 491.8 (3632.4–6039.1)	0.40	**< 0.001**	**< 0.001**	−1.1%	−2.9%	0.53	0.13	0.42
Pallidum	L	2323.2 ± 248.1 (1925.5–2979.1)	2343.2 ± 252.9 (1668.3–2995.8)	2290.7 ± 359.8 (1643.3–4507.8)	0.68	0.68	0.68	−1.2%	0.3%	0.49	0.88	0.53
	R	2385.1 ± 268.2 (1909.4–3021.0)	2368.4 ± 217.0 (1512.2–3130.0)	2337.0 ± 300.2 (1762.9–4039.6)	0.77	0.56	0.56	−2.3%	−1.1%	0.16	0.55	0.60
Putamen	L	6246.6 ± 622.1 (5028.7–8271.8)	6204.4 ± 673.9 (3648.3–7556.0)	5993.2 ± 610.1 (4615.8–8027.7)	0.35	0.16	0.35	−0.5%	−1.0%	0.77	0.59	0.81
	R	6079.5 ± 546.4 (5138.9–7342.9)	6104.19 ± 601.28 (4207.5–7740.3)	5948.3 ± 551.8 (4610.7–7355.5)	0.84	0.62	0.62	0.9%	−0.4%	0.55	0.81	0.52
Thalamus	L	9889.3 ± 738.3 (8141.0–11597.2)	9924.9 ± 767.5 (7524.0–11620.4)	9612.1 ± 777.0 (7817.9–11703.6)	0.91	0.12	0.12	−0.5%	−1.0%	0.62	0.41	0.75
	R	9511.1 ± 657.6 (8067.6–11014.0)	9574.1 ± 778.9 (7278.1–11175.8)	9258.3 ± 680.7 (7283.6–10978.8)	0.88	0.13	0.13	−0.5%	−1.1%	0.67	0.41	0.71
Variables	**Side**	**HC**	**Mild motor-predominant PD**	**Mild-diffuse PD**	**p: Mild motor-predominant PD *vs* HC**	**p: Mild-diffuse PD *vs* HC**	**p: Mild motor-predominant PD *vs* Mild-diffuse PD**	**Annualized mean rate of change (i.e. linear trend) Mild motor-predominant PD**	**Annualized mean rate of change (i.e. linear trend) Mild-diffuse PD**	**p for linear trend Mild motor-predominant PD**	**p for linear trend Mild-diffuse PD**	**p for differential trend Mild motor-predominant PD *vs* Mild-diffuse PD**
Amygdala	L	1791.0 ± 275.2 (1039.5–2397.2)	1822.4 ± 256.7 (1086.1–2507.3)	1869.1 ± 280.2 (969.3–2456.7)	0.55	0.47	0.55	−3.3%	−2.6%	0.37	0.48	0.90
	R	1846.3 ± 317.2 (858.1–2355.7)	1845.0 ± 304.7 (1183.0–2685.8)	1776.7 ± 374.3 (608.1–2533.3)	0.85	0.68	0.68	−8.2%	4.3%	0.12	0.44	0.06
Caudate	L	4298.6 ± 495.0 (2948.7–5576.8)	4363.5 ± 456.9 (3505.0–5213.6)	4246.5 ± 495.6 (3258.8–5427.3)	0.97	0.97	0.97	−1.2%	−0.2%	0.60	0.94	0.72
	R	4523.0 ± 426.6 (3515.5–5783.4)	4567.5 ± 490.4 (3763.2–5553.0)	4386.4 ± 583.8 (2355.0–5618.9)	0.88	0.44	0.44	−3.1%	1.1%	0.17	0.63	0.14
Hippocampus	L	4922.6 ± 507.4 (3806.4–6175.1)	5025.2 ± 453.2 (3875.4–6120.9)	4796.7 ± 472.5 (3897.6–5809.9)	0.46	0.31	0.21	−3.6%	−5.9%	0.12	**0.01**	0.46
	R	5120.9 ± 591.9 (3952.6–7879.1)	5308.4 ± 449.9 (4352.3–6123.4)	4985.7 ± 502.0 (2791.1–5631.2)	0.21	0.22	**0.04**	−2.4%	−4.4%	0.25	0.05	0.50
Pallidum	L	2323.2 ± 248.1 (1925.5–2979.1)	2320.5 ± 217.4 (1668.3–2711.9)	2366.0 ± 284.7 (1683.0–2995.8)	0.92	0.59	0.59	−3.0%	−3.3%	0.25	0.20	0.91
	R	2385.1 ± 268.2 (1909.4–3021.0)	2376.7 ± 169.4 (1936.9–2711.0)	2360.0 ± 257.7 (1512.2–3130.0)	0.98	0.90	0.90	−3.8%	−4.1%	0.11	0.09	0.92

(*continued on next page*)

Table 4 (*continued*)

Variables	Side	HC	Mild PD	Moderate-to-severe PD	p: Mild PD *vs* HC	p: Moderate-to-severe PD *vs* HC	p: Moderate-to-severe PD *vs* Mild PD	Annualized mean rate of change (i.e. linear trend) in Mild PD	Annualized mean rate of change (i.e. linear trend) in Moderate-to-severe PD	p for linear trend Mild PD	p for linear trend Moderate-to-severe PD	p for differential trend Mild PD *vs* Moderate-to-severe PD
Putamen	L	6246.6 ± 622.1 (5028.7–8271.8)	6272.5 ± 640.8 (4873.4–7544.8)	6136.2 ± 706.4 (3648.3–7556.0)	0.74	0.74	0.96	−3.0%	−0.9%	0.19	0.71	0.47
	R	6079.5 ± 546.4 (5138.9–7342.9)	6182.1 ± 643.5 (4816.9–7740.3)	6026.2 ± 552.4 (4207.48–7023.98)	0.94	0.94	0.94	0.6%	0.5%	0.78	0.82	0.97
Thalamus	L	9889.3 ± 738.3 (8141.0–11597.2)	10142.6 ± 856.2 (7524.0–11620.4)	9707.2 ± 601.7 (7918.6–10997.0)	0.28	0.28	0.12	−1.1%	−1.1%	0.50	0.52	0.91
	R	9511.1 ± 657.6 (8067.6–11014.0)	9801.0 ± 812.8 (7278.1–11175.8)	9347.1 ± 679.3 (7333.9–10341.2)	0.22	0.28	0.06	−1.8%	−0.6%	0.28	0.71	0.58

Values are reported as mean ± standard deviation (range) or number (%). Volumes are in mm^3. Differences between PD patients and healthy controls and between PD groups at baseline were assessed using one-way ANOVA (statistical contrasts). Annualized mean rate of changes (%) was obtained as the percentage difference between the variable mean at the end of follow-up (estimated by means of the regression slope found in a longitudinal model which included time as continuous variable) and the estimated variable mean at baseline. P-values were adjusted for multiple comparisons controlling the False Discovery Rate (FDR) at level 0.05 using Benjamini-Hochberg step-up procedure. Analyses were adjusted for age (baseline) and for age and LEDD change over time (longitudinal). Values in bold indicate statistically significant results. ***Abbreviations:*** *HC = healthy controls; L = left; PD = Parkinson's disease; R = right.*

Indeed, although no atrophy was observed at baseline in both mild clusters compared with controls, mild-diffuse PD patients were only slightly different from moderate-to-severe PD cases suggesting that the same amount of brain atrophy occurred in a shorter time span. In addition, longitudinal study showed that mild-diffuse patients, as moderate-to-severe PD cases, did not accumulate atrophy over one and two years, but had the most progressive GM atrophy pattern involving the cortex and the left hippocampus over a longer observation period. The most probable explanation is that the moderate-to-severe and mild-diffuse groups of patients had already accumulated atrophy at an earlier phase of the disease, thus achieving a sort of plateau. This hypothesis is supported by previous studies comparing de novo PD subjects with healthy controls over time, showing that PD subjects accumulated widespread GM atrophy of the cortex and hippocampus relative to healthy subjects in the early phase of the disease (Sampedro et al., 2019; Mollenhauer et al., 2016; Tessa et al., 2014). On the contrary, mild motor-predominant patients seem to show a more constant but less wide accumulation of atrophy each year. Our results on mild-diffuse patients are in line with a recent study subtyping *de novo* PD patients based on a comprehensive list of clinical manifestations and biomarkers which showed more brain atrophy in patients classified as "diffuse malignant" subtype (Fereshtehnejad et al., 2017).

Of note, previous MRI studies in mild PD cases have reported various brain structural results, ranging from the absence of cortical and subcortical alterations (Ibarretxe-Bilbao et al., 2012; Mak et al., 2015; Melzer et al., 2012; Weintraub et al., 2011) to widespread GM abnormalities in basal ganglia and fronto-temporal, parietal, and occipital areas relative to healthy controls (Lewis et al., 2016; Pereira et al., 2014). This heterogeneity is likely due to the variability of both the clinical samples (especially the presence/absence of cognitive impairment and other non-motor symptoms) and the MRI techniques. Together with previous evidence (Fereshtehnejad et al., 2017), our findings show that defining different subtypes of PD - early in the disease course - provides a unique opportunity to better understand the patterns of brain structural damage and to allow longitudinal assessment of disease progression.

Predicting patient trajectories is a challenge for clinicians. In this study, we demonstrated that cortical thinning at study entry and 1-year progression of atrophy predict subsequent long-term evolution of motor, cognitive, non-motor and mood dysfunctions in PD. Importantly, a greater involvement of the left inferior parietal lobe was a predictor of both motor and non-motor clinical evolution in all PD patients. The inferior parietal region has been involved in early mechanism of compensation in PD (Tahmasian et al., 2017). Its early and severe damage may presage a more rapid clinical progression in PD. Greater inferior parietal, orbitofrontal, precentral and anterior cingulate damage predicted the development of non-motor manifestations such as gastrointestinal, urinary, olfactory, orthostatic and sexual dysfunctions, indicating that the early presence of a diffuse neurodegenerative pattern identifies PD cases at high risk for non-motor symptomatology. Severe olfactory dysfunction was previously associated with atrophy of focal brain structures, including frontal and cingulate cortices (Baba et al., 2012). Our findings highlight the well-known central role of frontal and medial occipito-temporal structural damage in determining cognitive impairment in PD patients (Compta et al., 2013; Garcia-Diaz et al., 2018; Gee et al., 2017; Gorges et al., 2020; Hanganu et al., 2014; Melzer et al., 2015; Ramírez–Ruiz et al., 2005; Sampedro et al., 2019). These results are in line with theories regarding the etiology of cognitive impairment in PD, which include striatal dysfunction that results in secondary effects on the frontal lobe, primary frontal lobe dysfunction, and more widespread cortical dysfunction secondary to global neurotransmitter system deficits. Finally, mood alterations in the early phase of the disease, including anxiety, depression and apathy, were predicted by the cortical thinning of the middle frontal and postcentral regions, confirming the role of fronto-parietal regions in mood control as suggested by previous cross-

Table 5
Baseline and baseline + 1-year change MRI prediction model of the clinical evolution over the whole follow-up in PD subtypes.

	MOTOR GCO						NON-MOTOR GCO					
	Baseline MRI	**Slope (p-value)**	**Adj R^2 value**	**Baseline + 1-year change (delta) MRI**	**Slope of delta MRI (p-value)**	**Adj R^2 value**	**Baseline MRI**	**Slope (p-value)**	**Adj R^2 value**	**Baseline + 1-year change (delta) MRI**	**Slope of delta MRI (p-value)**	**Adj R^2 value**
All PD	L inferior parietal	−1.62 (p = **0.02**)	0.42	–	–	–	L inferior parietal	−2.51 (**p = 0.01**)	0.27	–	–	–
Moderate-to-severe PD	R medial orbitofr	−1.37 (p = **0.03**)	0.31	–	–	–	R rostral anterior cingulate	−1.07 (p = 0.06)	0.13	–	–	–
MildPD	L isthmus cingulate	−1.56 (p = **0.003**)	0.10	–	–	–	L inferior parietal + R medial orbitofr	−2.31 (p = 0.06) and −1.50 (p = 0.08)	0.20	–	–	–
Mild motor-predominant PD	–	–	–	–	–	–	R medial orbitofr + L precentral	−2.38 (p = **0.02**) and −1.71 (p = 0.06)	0.39	–	–	–
Mild-diffuse PD	–	–	–	L inferior temporal	6.27 (p = 0.004)	0.17	L rostral anterior cingulate	1.65 (**p = 0.04**)	0.11	L inferior temporal + R medial orbitofr	6.07 (p = **0.04**) and 4.57 (p = **0.03**)	0.24
	COGNITIVE GCO						**MOOD GCO**					
All PD	–	–	–	L postcent	−3.02 (p = **0.002**)	0.42	–	–	–	–	–	–
Moderate-to-severe PD	R medial orbitofr	1.54 (p = **0.03**)	0.35	L medial orbitofr	−3.83 (p = **0.05**)	0.32	–	–	–	–	–	–
Mild PD	–	–	–	R lingual	3.12 (p = **0.03**)	0.30	–	–	–	–	–	–
Mild motor-predominant PD	–	–	–	–	–	–	R rostral middle frontal	−4.19 (p < **0.001**)	0.22	L postcent	−4.66 (p = **0.02**)	0.05
Mild-diffuse PD	R precentral	−1.98 (p = **0.03**)	0.27	R lingual	4.54 (p = **0.02**)	0.30	L pars opercul	4.35 (p = **0.02**)	0.12	–	–	–

Linear regression models were built to assess the association between baseline MRI measures (cortical thickness/grey matter volumes) or baseline + 1-year change MRI measures and GCOs. Each GCO was considered as the dependent variable into each model, which also included age, baseline LEDD, individual follow-up duration, and baseline MRI measures or baseline + 1-year change of MRI measures as covariates (independent variables). Both regression slope (along with its p-value) of MRI measures included into the models and adjusted R^2 goodness of fit statistic were estimated for each model at issue and for each PD subtype, separately. Values in bold indicate statistically significant results. ***Abbreviations:*** *GCO = global composite outcome; HC = healthy controls; L = left; Orbitofr = orbitofrontal; Opercul = opercularis; PD = Parkinson's disease; Postcent = postcentral; R = right.*

sectional (Wee et al., 2016) and longitudinal (Hanganu et al., 2017) studies.

Finally, a consideration should be also reserved to the left hemispheric lateralization seen in our results. It is already well known in the literature that the left hemisphere is more susceptible to damage in PD (Claassen et al., 2016) and in general in neurodegenerative diseases such as Alzheimer's disease, behavioral fronto-temporal dementia and non-fluent or semantic primary progressive aphasia (Janke et al., 2001; Rohrer et al., 2012; Tomlinson et al., 2010; Whitwell et al., 2013). To date, the etiology of this phenomenon is still unclear, but several reasons have been discussed including a greater vulnerability of the dominant hemisphere and disease specific issues. Indeed, the left hemisphere is recognized to be highly specialized for motor planning and organization of complex movements/ experienced actions, motor learning and language processing (Serrien et al., 2006; Serrien and Sovijärvi-Spapé, 2015), besides being more frequently the dominant hemisphere. Finally, left cortical atrophy could reflect the underlying nigrostriatal failure considering that the nigrostriatal system in PD seems to be firstly involved in its left side (Postuma and Dagher, 2006; van der Hoorn et al., 2012).

This study is not without limitations. First, we do not have longitudinal MRI data in healthy controls and this is a serious concern. Thus, even if our analyses are corrected for age, we cannot ignore that part of the structural changes we observed in patients was related to aging effects. However, our findings demonstrated different patterns of atrophy accumulation in PD subtypes with a similar age that are in line with previous studies including longitudinal comparison of PD patients with healthy controls. Second, the interpretation of differences over time among groups should be considered carefully because it is focused mainly on within group changes while most group × time interactions were not significant. Third, we used a 1.5 T MRI scanner, which is characterized by a lower spatial resolution compared with higher field strength scanners. Fourth, several studies have attempted to divide PD patients into clusters (Greenland et al., 2019). Our data-driven subtyping needs to be validated in independent cohorts before it can be translated in real-life practical application. Integration of neuroimaging data in the cluster solution may also improve prognostic stratification of patients (Uribe et al., 2016). Fifth, the attrition rate was relatively high in moderate-to-severe PD patients, which is however in line with previous studies (Uribe et al., 2019; Sarasso et al., 2020).

In conclusion, our data suggest trajectories of brain structural changes according to PD subtypes and prognosis. Cortical and subcortical atrophy is accelerated early after the disease onset and becomes prominent in later stages of disease suggesting that structural MRI may be useful for monitoring and predicting disease progression.

Declaration of interest

M. Filippi is Editor-in-Chief of the Journal of Neurology; received compensation for consulting services and/or speaking activities from Bayer, Biogen Idec, Merck-Serono, Novartis, Roche, Sanofi Genzyme, Takeda, and Teva Pharmaceutical Industries; and receives research support from Biogen Idec, Merck-Serono, Novartis, Roche, Teva Pharmaceutical Industries, Italian Ministry of Health, Fondazione Italiana Sclerosi Multipla, and ARiSLA (Fondazione Italiana di Ricerca per la SLA). E. Sarasso, N. Piramide, I. Stankovic, S. Basaia, A. Fontana, A. Tomic, and V. Markovic report no disclosures. T. Stojkovic has received speaker honoraria from Actavis and Alzheimer's Association International Research Grant. E. Stefanova has received speaker honoraria from Actavis. V.S. Kostic has received speaker honoraria from Actavis and Solveo. F. Agosta is Section Editor of NeuroImage: Clinical; has received speaker honoraria from Philips, Novartis and Biogen Idec; and receives or has received research supports from the Italian Ministry of Health, AriSLA (Fondazione Italiana di Ricerca per la SLA), and the European Research Council.

CRediT authorship contribution statement

Massimo Filippi: Conceptualization, Methodology, Project administration, Resources, Supervision, Writing - original draft, Writing - review & editing. **Elisabetta Sarasso:** Formal analysis, Writing - review & editing. **Noemi Piramide:** Formal analysis, Writing - review & editing. **Tanja Stojkovic:** Investigation, Formal analysis, Writing - review & editing. **Iva Stankovic:** Investigation, Formal analysis, Writing - review & editing. **Silvia Basaia:** Formal analysis, Writing - review & editing. **Andrea Fontana:** Formal analysis, Writing - review & editing. **Aleksandra Tomic:** Investigation, Formal analysis, Writing - review & editing. **Vladana Markovic:** Investigation, Formal analysis, Writing - review & editing. **Elka Stefanova:** Investigation, Formal analysis, Writing - review & editing. **Vladimir S. Kostic:** Conceptualization, Formal analysis, Writing - review & editing, Funding acquisition, Resources. **Federica Agosta:** Conceptualization, Formal analysis, Writing - original draft, Writing - review & editing, Funding acquisition, Resources.

Acknowledgments

The authors thank the patients and their families for the time and effort they dedicated to the research.

Funding

This work was supported by the Ministry of Education, Science, and Technological Development of the Republic of Serbia [grant number #175090] and the Italian Ministry of Health [grant number # RF-2018-12366746].

Appendix A. Supplementary data

Supplementary data to this article can be found online at https://doi.org/10.1016/j.nicl.2020.102374.

References

Agosta, F., Canu, E., Stojković, T., Pievani, M., Tomić, A., Sarro, L., Dragašević, N., Copetti, M., Comi, G., Kostić, V.S., Filippi, M., 2013a. The topography of brain damage at different stages of Parkinson's disease: in Vivo PD Staging Using MRI. Hum. Brain Mapp 34 (11), 2798–2807.

Agosta, F., Kostic, V.S., Davidovic, K., Kresojević, N., Sarro, L., Svetel, M., Stanković, I., Comi, G., Klein, C., Filippi, M., 2013b. White matter abnormalities in Parkinson's disease patients with glucocerebrosidase gene mutations: WM Alterations in GBA-Associated pd. Mov. Disord. 28 (6), 772–778.

Baba, T., Kikuchi, A., Hirayama, K., Nishio, Y., Hosokai, Y., Kanno, S., Hasegawa, T., Sugeno, N., Konno, M., Suzuki, K., Takahashi, S., Fukuda, H., Aoki, M., Itoyama, Y., Mori, E., Takeda, A., 2012. Severe olfactory dysfunction is a prodromal symptom of dementia associated with Parkinson's disease: a 3 year longitudinal study. Brain 135, 161–169.

Bernal-Rusiel, J.L., Greve, D.N., Reuter, M., Fischl, B., Sabuncu, M.R., Alzheimer's Disease Neuroimaging, I., 2013. Statistical analysis of longitudinal neuroimage data with Linear Mixed Effects models. Neuroimage 66, 249–260.

Braak, H., Bohl, J.R., Muller, C.M., Rub, U., de Vos, R.A., Del Tredici, K., 2006. Stanley Fahn Lecture 2005: the staging procedure for the inclusion body pathology associated with sporadic Parkinson's disease reconsidered. Mov. Disord. 21, 2042–2051.

Camicioli, R., Sabino, J., Gee, M., Bouchard, T., Fisher, N., Hanstock, C., Emery, D., Martin, W.R.W., 2011. Ventricular Dilatation and Brain Atrophy in Patients with Parkinson's Disease with Incipient Dementia. Mov. Disord. 26, 1443–1450.

Campabadal, A., Uribe, C., Segura, B., Baggio, H.C., Abos, A., Garcia-Diaz, A.I., Marti, M. J., Valldeoriola, F., Compta, Y., Bargallo, N., Junque, C., 2017. Brain correlates of progressive olfactory loss in Parkinson's disease. Parkinsonism Relat. Disord. 41, 44–50.

Caspell-Garcia, C., Simuni, T., Tosun-Turgut, D., Wu, I.W., Zhang, Y., Nalls, M., Singleton, A., Shaw, L.A., Kang, J.H., Trojanowski, J.Q., Siderowf, A., Coffey, C., Lasch, S., Aarsland, D., Burn, D., Chahine, L.M., Espay, A.J., Foster, E.D., Hawkins, K.A., Litvan, I., Richard, I., Weintraub, D., Parkinson's Progression Markers, I., 2017. Multiple modality biomarker prediction of cognitive impairment in prospectively followed de novo Parkinson disease. PLoS One 12, e0175674.

Chaudhuri, K.R., Martinez-Martin, P., Schapira, A.H., Stocchi, F., Sethi, K., Odin, P., Brown, R.G., Koller, W., Barone, P., MacPhee, G., Kelly, L., Rabey, M., MacMahon, D., Thomas, S., Ondo, W., Rye, D., Forbes, A., Tluk, S., Dhawan, V., Bowron, A., Williams, A.J., Olanow, C.W., 2006. International multicenter pilot study of the first

comprehensive self-completed nonmotor symptoms questionnaire for Parkinson's disease: the NMSQuest study. Mov. Disord. 21, 916–923.
Claassen, Daniel O., McDonell, Katherine E., Donahue, Manus, Rawal, Shiv, Wylie, Scott A., Neimat, Joseph S., Kang, Hakmook, Hedera, Peter, Zald, David, Landman, Bennett, Dawant, Benoit, Rane, Swati, 2016. Cortical asymmetry in Parkinson's disease: early susceptibility of the left hemisphere. Brain Behav. 6 (12), e00573. https://doi.org/10.1002/brb3.2016.6.issue-1210.1002/brb3.573.
Compta, Y., Pereira, J.B., Rios, J., Ibarretxe-Bilbao, N., Junque, C., Bargallo, N., Camara, A., Buongiorno, M., Fernandez, M., Pont-Sunyer, C., Marti, M.J., 2013. Combined dementia-risk biomarkers in Parkinson's disease: a prospective longitudinal study. Parkinsonism Relat. Disord. 19, 717–724.
Dale, Anders M., Fischl, Bruce, Sereno, Martin I., 1999. Cortical surface-based analysis. NeuroImage 9 (2), 179–194.
Desikan, Rahul S., Ségonne, Florent, Fischl, Bruce, Quinn, Brian T., Dickerson, Bradford C., Blacker, Deborah, Buckner, Randy L., Dale, Anders M., Maguire, R. Paul, Hyman, Bradley T., Albert, Marilyn S., Killiany, Ronald J., 2006. An automated labeling system for subdividing the human cerebral cortex on MRI scans into gyral based regions of interest. NeuroImage 31 (3), 968–980.
Emre, Murat, Aarsland, Dag, Brown, Richard, Burn, David J., Duyckaerts, Charles, Mizuno, Yoshikino, Broe, Gerald Anthony, Cummings, Jeffrey, Dickson, Dennis W., Gauthier, Serge, Goldman, Jennifer, Goetz, Christopher, Korczyn, Amos, Lees, Andrew, Levy, Richard, Litvan, Irene, McKeith, Ian, Olanow, Warren, Poewe, Werner, Quinn, Niall, Sampaio, Christina, Tolosa, Eduardo, Dubois, Bruno, 2007. Clinical diagnostic criteria for dementia associated with Parkinson's disease. Mov. Disord. 22 (12), 1689–1707.
Fereshtehnejad, S.M., Zeighami, Y., Dagher, A., Postuma, R.B., 2017. Clinical criteria for subtyping Parkinson's disease: biomarkers and longitudinal progression. Brain 140, 1959–1976.
Filippi, M., Basaia, S., Sarasso, E., Stojkovic, T., Stankovic, I., Fontana, A., Tomic, A., Piramide, N., Stefanova, E., Markovic, V., Kostic, V.S., Agosta, F., 2020. Longitudinal brain connectivity changes and clinical evolution in Parkinson's disease. Molecular psychiatry.
Filippi, M., Elisabetta, S., Piramide, N., Agosta, F., 2018. Functional MRI in Idiopathic Parkinson's Disease. Int. Rev. Neurobiol. 141, 439–467.
Fischl, B., Dale, A.M., 2000. Measuring the thickness of the human cerebral cortex from magnetic resonance images. Proc. Natl. Acad. Sci. U S A 97, 11050–11055.
Foo, H., Mak, E., Yong, T.T., Wen, M.C., Chander, R.J., Au, W.L., Sitoh, Y.Y., Tan, L.C., Kandiah, N., 2017. Progression of subcortical atrophy in mild Parkinson's disease and its impact on cognition. Eur. J. Neurol. 24, 341–348.
Garcia-Diaz, A.I., Segura, B., Baggio, H.C., Uribe, C., Campabadal, A., Abos, A., Marti, M. J., Valldeoriola, F., Compta, Y., Bargallo, N., Junque, C., 2018. Cortical thinning correlates of changes in visuospatial and visuoperceptual performance in Parkinson's disease: a 4-year follow-up. Parkinsonism Relat. Disord. 46, 62–68.
Gee, Myrlene, Dukart, Juergen, Draganski, Bogdan, Wayne Martin, WR, Emery, Derek, Camicioli, Richard, 2017. Regional volumetric change in Parkinson's disease with cognitive decline. J. Neurol. Sci. 373, 88–94.
Giladi, N., Shabtai, H., Simon, E.S., Biran, S., Tal, J., Korczyn, A.D., 2000. Construction of freezing of gait questionnaire for patients with Parkinsonism. Parkinsonism Related Disorders 6 (3), 165–170.
Gorges, Martin, Kunz, Martin S., Müller, Hans-Peter, Liepelt-Scarfone, Inga, Storch, Alexander, Dodel, Richard, Hilker-Roggendorf, Rüdiger, Berg, Daniela, Kalbe, Elke, Braak, Heiko, Del Tredici, Kelly, Baudrexel, Simon, Huppertz, Hans-Jürgen, Kassubek, Jan, 2020. Longitudinal brain atrophy distribution in advanced Parkinson's disease: What makes the difference in “cognitive status” converters? Hum. Brain Mapp 41 (6), 1416–1434.
Greenland, Julia C., Williams-Gray, Caroline H., Barker, Roger A., 2019. The clinical heterogeneity of Parkinson's disease and its therapeutic implications. Eur. J. Neurosci. 49 (3), 328–338.
Hanganu, A., Bedetti, C., Degroot, C., Mejia-Constain, B., Lafontaine, A.L., Soland, V., Chouinard, S., Bruneau, M.A., Mellah, S., Belleville, S., Monchi, O., 2014. Mild cognitive impairment is linked with faster rate of cortical thinning in patients with Parkinson's disease longitudinally. Brain 137, 1120–1129.
Hanganu, A., Bedetti, C., Jubault, T., Gagnon, J.F., Mejia-Constain, B., Degroot, C., Lafontaine, A.L., Chouinard, S., Monchi, O., 2013. Mild cognitive impairment in patients with Parkinson's disease is associated with increased cortical degeneration. Movement disorders : official journal of the Movement Disorder Society 28, 1360–1369.
Hanganu, A., Bruneau, M.A., Degroot, C., Bedetti, C., Mejia-Constain, B., Lafontaine, A.L., Chouinard, S., Monchi, O., 2017. Depressive symptoms in Parkinson's disease correlate with cortical atrophy over time. Brain Cogn. 111, 127–133.
Hoehn, M.M., Yahr, M.D., 1967. Parkinsonism: onset, progression and mortality. Neurology 17, 427–442.
Ibarretxe-Bilbao, N., Junque, C., Segura, B., Baggio, H.C., Marti, M.J., Valldeoriola, F., Bargallo, N., Tolosa, E., 2012. Progression of cortical thinning in early Parkinson's disease. Mov. Disord. 27, 1746–1753.
Ibarretxe-Bilbao, N., Ramirez-Ruiz, B., Junque, C., Marti, M.J., Valldeoriola, F., Bargallo, N., Juanes, S., Tolosa, E., 2010. Differential progression of brain atrophy in Parkinson's disease with and without visual hallucinations. J. Neurol. Neurosurg. Psychiatry 81, 650–657.
Janke, Andrew L., Zubicaray, Greig de, Rose, Stephen E., Griffin, Mark, Chalk, Jonathan B., Galloway, Graham J., 2001. 4D deformation modeling of cortical disease progression in Alzheimer's dementia. Magn. Reson. Med. 46 (4), 661–666.
Lewis, Mechelle M., Du, Guangwei, Lee, Eun-Young, Nasralah, Zeinab, Sterling, Nicholas W., Zhang, Lijun, Wagner, Daymond, Kong, Lan, Tröster, Alexander I., Styner, Martin, Eslinger, Paul J., Mailman, Richard B., Huang, Xuemei, 2016. The pattern of gray matter atrophy in Parkinson’s disease differs in cortical and subcortical regions. J. Neurol. 263 (1), 68–75.
Mak, Elijah, Su, Li, Williams, Guy B., Firbank, Michael J., Lawson, Rachael A., Yarnall, Alison J., Duncan, Gordon W., Mollenhauer, Brit, Owen, Adrian M., Khoo, Tien K., Brooks, David J., Rowe, James B., Barker, Roger A., Burn, David J., O'Brien, John T., 2017. Longitudinal whole-brain atrophy and ventricular enlargement in non-demented Parkinson's disease. Neurobiol. Aging 55, 78–90.
Mak, Elijah, Su, Li, Williams, Guy B., Firbank, Michael J., Lawson, Rachael A., Yarnall, Alison J., Duncan, Gordon W., Owen, Adrian M., Khoo, Tien K., Brooks, David J., Rowe, James B., Barker, Roger A., Burn, David J., O'Brien, John T., 2015. Baseline and longitudinal grey matter changes in newly diagnosed Parkinson’s disease: ICICLE-PD study. Brain 138 (10), 2974–2986.
Melzer, T.R., Myall, D.J., MacAskill, M.R., Pitcher, T.L., Livingston, L., Watts, R., Keenan, R.J., Dalrymple-Alford, J.C., Anderson, T.J., 2015. Tracking Parkinson's Disease over One Year with Multimodal Magnetic Resonance Imaging in a Group of Older Patients with Moderate Disease. PLoS One 10, e0143923.
Melzer, Tracy R, Watts, Richard, MacAskill, Michael R, Pitcher, Toni L, Livingston, Leslie, Keenan, Ross J, Dalrymple-Alford, John C, Anderson, Tim J, 2012. Grey matter atrophy in cognitively impaired Parkinson's disease. J. Neurol. Neurosurg. Psychiatry 83 (2), 188–194.
Mestre, Tiago A., Eberly, Shirley, Tanner, Caroline, Grimes, David, Lang, Anthony E., Oakes, David, Marras, Connie, 2018. Reproducibility of data-driven Parkinson's disease subtypes for clinical research. Parkinsonism Related Disorders 56, 102–106.
Mollenhauer, Brit, Zimmermann, Johannes, Sixel-Döring, Friederike, Focke, Niels K., Wicke, Tamara, Ebentheuer, Jens, Schaumburg, Martina, Lang, Elisabeth, Trautmann, Ellen, Zetterberg, Henrik, Taylor, Peggy, Friede, Tim, Trenkwalder, Claudia, 2016. Monitoring of 30 marker candidates in early Parkinson disease as progression markers. Neurology 87 (2), 168–177.
Movement Disorder Society Task Force on Rating Scales for Parkinson's, D., 2003. The Unified Parkinson's Disease Rating Scale (UPDRS): status and recommendations. Mov. Disord. 18, 738–750.
Nürnberger, Lucas, Gracien, René-Maxime, Hok, Pavel, Hof, Stephanie-Michelle, Rüb, Udo, Steinmetz, Helmuth, Hilker, Rüdiger, Klein, Johannes C., Deichmann, Ralf, Baudrexel, Simon, 2017. Longitudinal changes of cortical microstructure in Parkinson's disease assessed with T1 relaxometry. NeuroImage: Clinical 13, 405–414.
Pereira, J.B., Svenningsson, P., Weintraub, D., Bronnick, K., Lebedev, A., Westman, E., Aarsland, D., 2014. Initial cognitive decline is associated with cortical thinning in early Parkinson disease. Neurology 82, 2017–2025.
Postuma, R.B., Dagher, A., 2006. Basal ganglia functional connectivity based on a meta-analysis of 126 positron emission tomography and functional magnetic resonance imaging publications. Cereb Cortex 16, 1508–1521.
Qian, Elizabeth, Huang, Yue, 2019. Subtyping of Parkinson’s disease - where are we up to? Aging Disease 10 (5), 1130. https://doi.org/10.14336/AD.2019.0112.
Ramirez-Ruiz, B., Marti, M.J., Tolosa, E., Bartres-Faz, D., Summerfield, C., Salgado-Pineda, P., Gomez-Anson, B., Junque, C., 2005. Longitudinal evaluation of cerebral morphological changes in Parkinson's disease with and without dementia. J. Neurol. 252, 1345–1352.
Reuter, M., Rosas, H.D., Fischl, B., 2010. Highly accurate inverse consistent registration: a robust approach. Neuroimage 53, 1181–1196.
Rohrer, Jonathan D., Clarkson, Matthew J., Kittus, Raivo, Rossor, Martin N., Ourselin, Sebastien, Warren, Jason D., Fox, Nick C., 2012. Rates of hemispheric and lobar atrophy in the language variants of frontotemporal lobar degeneration. JAD 30 (2), 407–411.
Sampedro, F., Martinez-Horta, S., Marin-Lahoz, J., Pagonabarraga, J., Kulisevsky, J., 2019. Longitudinal intracortical diffusivity changes in de-novo Parkinson's disease: A promising imaging biomarker. Parkinsonism Relat. Disord. 68, 22–25.
Sarasso, E., Agosta, F., Piramide, N., Filippi, M., 2020. Progression of grey and white matter brain damage in Parkinson's disease: a critical review of structural MRI literature. J. Neurol.
Serrien, Deborah J., Ivry, Richard B., Swinnen, Stephan P., 2006. Dynamics of hemispheric specialization and integration in the context of motor control. Nat. Rev. Neurosci. 7 (2), 160–166.
Serrien, Deborah J., Sovijärvi-Spapé, Michiel M., 2015. Hemispheric asymmetries and the control of motor sequences. Behav. Brain Res. 283, 30–36.
Sterling, Nicholas W., Wang, Ming, Zhang, Lijun, Lee, Eun-Young, Du, Guangwei, Lewis, Mechelle M., Styner, Martin, Huang, Xuemei, 2016. Stage-dependent loss of cortical gyrification as Parkinson disease “unfolds”. Neurology 86 (12), 1143–1151.
Stiasny-Kolster, Karin, Mayer, Geert, Schäfer, Sylvia, Möller, Jens Carsten, Heinzel-Gutenbrunner, Monika, Oertel, Wolfgang H., 2007. The REM sleep behavior disorder screening questionnaire-a new diagnostic instrument. Mov. Disord. 22 (16), 2386–2393.
Stojkovic, Tanja, Stefanova, Elka, Soldatovic, Ivan, Markovic, Vladana, Stankovic, Iva, Petrovic, Igor, Agosta, Federica, Galantucci, Sebastiano, Filippi, Massimo, Kostic, Vladimir, 2018. Exploring the relationship between motor impairment, vascular burden and cognition in Parkinson’s disease. J. Neurol. 265 (6), 1320–1327.
Tahmasian, Masoud, Eickhoff, Simon B., Giehl, Kathrin, Schwartz, Frank, Herz, Damian M., Drzezga, Alexander, van Eimeren, Thilo, Laird, Angela R., Fox, Peter T., Khazaie, Habibolah, Zarei, Mojtaba, Eggers, Carsten, Eickhoff, Claudia R., 2017. Resting-state functional reorganization in Parkinson's disease: an activation likelihood estimation meta-analysis. Cortex 92, 119–138.
Tessa, Carlo, Lucetti, Claudio, Giannelli, Marco, Diciotti, Stefano, Poletti, Michele, Danti, Sabrina, Baldacci, Filippo, Vignali, Claudio, Bonuccelli, Ubaldo, Mascalchi, Mario, Toschi, Nicola, 2014. Progression of brain atrophy in the early stages of Parkinson's disease: a longitudinal tensor-based morphometry study in de novo patients without cognitive impairment. Hum. Brain Mapp. 35 (8), 3932–3944.
Tomlinson, Claire L., Stowe, Rebecca, Patel, Smitaa, Rick, Caroline, Gray, Richard, Clarke, Carl E., 2010. Systematic review of levodopa dose equivalency reporting in

Parkinson's disease: Systematic Review of LED Reporting in PD. Mov. Disord. 25 (15), 2649–2653.
Uribe, C., Segura, B., Baggio, H.C., Abos, A., Garcia-Diaz, A.I., Campabadal, A., Marti, M. J., Valldeoriola, F., Compta, Y., Bargallo, N., Junque, C., 2019. Progression of Parkinson's disease patients' subtypes based on cortical thinning: 4-year follow-up. Parkinsonism Relat. Disord.
Uribe, C., Segura, B., Baggio, H.C., Abos, A., Marti, M.J., Valldeoriola, F., Compta, Y., Bargallo, N., Junque, C., 2016. Patterns of cortical thinning in nondemented Parkinson's disease patients. Mov. Disord. 31, 699–708.
van der Hoorn, Anouk, Burger, Huibert, Leenders, Klaus L., de Jong, Bauke M., 2012. Handedness correlates with the dominant Parkinson side: a systematic review and meta-analysis. Mov. Disord. 27 (2), 206–210.
van Rooden, Stephanie M., Heiser, Willem J., Kok, Joost N., Verbaan, Dagmar, van Hilten, Jacobus J., Marinus, Johan, 2010. The identification of Parkinson's disease subtypes using cluster analysis: a systematic review. Mov. Disord. 25 (8), 969–978.
Wee, N., Wen, M.C., Kandiah, N., Chander, R.J., Ng, A., Au, W.L., Tan, L.C., 2016. Neural correlates of anxiety symptoms in mild Parkinson's disease: a prospective longitudinal voxel-based morphometry study. J. Neurol. Sci. 371, 131–136.
Weintraub, D., Doshi, J., Koka, D., Davatzikos, C., Siderowf, A.D., Duda, J.E., Wolk, D.A., Moberg, P.J., Xie, S.X., Clark, C.M., 2011. Neurodegeneration across stages of cognitive decline in Parkinson disease. Arch. Neurol. 68, 1562–1568.
Weintraub, Daniel, Hoops, Staci, Shea, Judy A., Lyons, Kelly E., Pahwa, Rajesh, Driver-Dunckley, Erika D., Adler, Charles H., Potenza, Marc N., Miyasaki, Janis, Siderowf, Andrew D., Duda, John E., Hurtig, Howard I., Colcher, Amy, Horn, Stacy S., Stern, Matthew B., Voon, Valerie, 2009. Validation of the questionnaire for impulsive-compulsive disorders in Parkinson's disease: ICD Questionnaire for Parkinson's Disease. Mov. Disord. 24 (10), 1461–1467.
Whitwell, Jennifer L., Xu, Jia, Mandrekar, Jay, Boeve, Bradley F., Knopman, David S., Parisi, Joseph E., Senjem, Matthew L., Dickson, Dennis W., Petersen, Ronald C., Rademakers, Rosa, Jack Jr., Clifford R., Josephs, Keith A., 2013. Frontal asymmetry in behavioral variant frontotemporal dementia: clinicoimaging and pathogenetic correlates. Neurobiol. Aging 34 (2), 636–639.
Zhou, Cheng, Guan, Xiao-Jun, Guo, Tao, Zeng, Qiao-Ling, Gao, Ting, Huang, Pei-Yu, Xuan, Min, Gu, Quan-Quan, Xu, Xiao-Jun, Zhang, Min-Ming, 2020. Progressive brain atrophy in Parkinson's disease patients who convert to mild cognitive impairment. CNS Neurosci. Ther. 26 (1), 117–125.